



UNIVERSITY OF LEEDS

This is a repository copy of *Numerical and experimental evaluation on the pooled effect of waste cooking oil biodiesel/diesel blends and exhaust gas recirculation in a twin-cylinder diesel engine*.

White Rose Research Online URL for this paper:
<https://eprints.whiterose.ac.uk/170725/>

Version: Accepted Version

Article:

Balasubramanian, D, Hoang, AT, Papla Venugopal, I et al. (3 more authors) (2021) Numerical and experimental evaluation on the pooled effect of waste cooking oil biodiesel/diesel blends and exhaust gas recirculation in a twin-cylinder diesel engine. *Fuel*, 287. 119815. ISSN 0016-2361

<https://doi.org/10.1016/j.fuel.2020.119815>

© 2020, Elsevier Ltd. This manuscript version is made available under the CC-BY-NC-ND 4.0 license <http://creativecommons.org/licenses/by-nc-nd/4.0/>.

Reuse

This article is distributed under the terms of the Creative Commons Attribution-NonCommercial-NoDerivs (CC BY-NC-ND) licence. This licence only allows you to download this work and share it with others as long as you credit the authors, but you can't change the article in any way or use it commercially. More information and the full terms of the licence here: <https://creativecommons.org/licenses/>

Takedown

If you consider content in White Rose Research Online to be in breach of UK law, please notify us by emailing eprints@whiterose.ac.uk including the URL of the record and the reason for the withdrawal request.



eprints@whiterose.ac.uk
<https://eprints.whiterose.ac.uk/>

1 **NUMERICAL AND EXPERIMENTAL EVALUATION ON THE POOLED**
2 **EFFECT OF WASTE COOKING OIL BIODIESEL/DIESEL BLENDS AND**
3 **EXHAUST GAS RECIRCULATION IN A TWIN-CYLINDER DIESEL**
4 **ENGINE**

5 ***Dhinesh Balasubramanian ^{*a}, Hoang Anh Tuan ^{*b}, Inbanaathan Papla Venugopal ^{a,c},***
6 ***Arunprasad Shanmugam ^c, Jianbing Gao ^d, Tanakorn Wongwuttanasatian ^{e,f}***

7 ^{*a} Department of Mechanical Engineering, Mepco Schlenk Engineering College, Sivakasi, India.

8 ^{*b} Ho Chi Minh City University of Technology (HUTECH), Ho Chi Minh City, Viet Nam

9 ^c Department of Production Engineering, Sri Sairam Engineering College, Chennai.

10 ^d Institute of Transport Studies (ITS), University of Leeds, United Kingdom.

11 ^e Mechanical Engineering, Faculty of Engineering, Khon Kaen University, Khon Kaen, Thailand

12 ^f Center for Alternative Energy Research and Development, Khon Kaen University, Khon Kaen, Thailand

13 **Corresponding Author - Email ID – dhineshbala91@gmail.com, hatuan@hutech.edu.vn**

14 **Abstract**

15 Nowadays, worldwide, many countries are engaged in reducing the vehicular exhaust
16 emissions from diesel engines as diesel engines are the main source of power in various transport
17 applications. Biofuels obtained from various feedstocks serve as a better alternative fuel in CI
18 engines because of its emission reducing capabilities. The major drawback in the usage of biofuels
19 in CI engine is the rise in the formation of nitrogen oxides which would be harmful to human health.
20 WCO biofuel was processed using trans-esterification technique and the contents available were
21 analyzed using gas chromatography mass .spectroscopy (GCMS). Four different blends, namely B100,

22 B60, B40, and B20 were made. The physio-chemical properties of the prepared test fuels were
23 identified using ASTM standards. The investigation on the characterisation of performance,
24 combustion, sound and emission of the test engine was done. Fuel combustion modeling was done
25 using ANSYS Fluent for diesel, WCO biofuel and best suited blend obtained from experimental
26 results. From both the simulated and the experimental results, it was found that B20 blend fuel
27 would be best suited to the test engine with a maximum reduction of 17% in unburned
28 hydrocarbon (HC), 30% in carbonmonoxide (CO), 14.08% in smoke, 7.35% in carbondioxide (CO₂)
29 and 16.46% increase in NO_x emission respectively. With an intention to reduce NO_x emission in the
30 selected B20 blend fuel, EGR at three rates, namely (5%, 10%, and 15%) were utilized. Again, the
31 experiments were conducted with varying EGR rates for B20 blend fuel. A good percentage of
32 reduction in NO_x was obtained with increase in EGR rates. But other emissions like CO, HC, smoke,
33 and CO₂ emissions were found to increase with rise in EGR rates. Thus, a comparison was made
34 with three rates of EGR emission values with all types of test fuels to optimize the EGR rate leading
35 into the inlet charge. 10% EGR rate gave a maximum reduction of 16.34% in NO_x emission without
36 affecting much in the emissions like HC, CO, Smoke, and CO₂ along with a small drop in
37 performance.

38 **Keywords:** WCO biofuel, Diesel, Exhaust gas recirculation, Performance, Combustion, Emission.

39

40 **1. Introduction**

41 In recent days compression ignition (CI) engines have been more popular than gasoline engines
42 because of their low cost in maintenance, high power, fuel economy and high range of torque. In
43 the last century, it became a predominant power application in transport industry and also in
44 powering the farm equipment. Though the emissions from diesel are named to be carcinogenic, it is

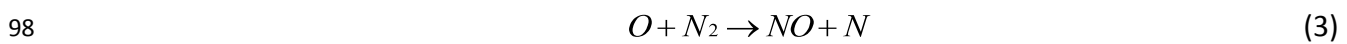
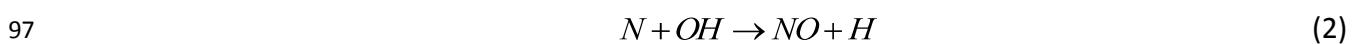
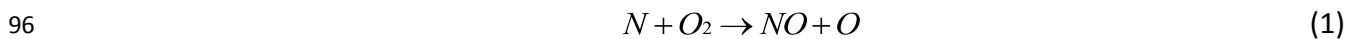
45 still better than gasoline engines as far as the amount of emission emitted to the atmosphere is
46 concerned. The emissions from the diesel engines serve as a source of global warming that has
47 deteriorated the health of human beings more in recent times. So, this prompted many researchers
48 to concentrate on bio-derived fuels as an alternative to the diesel fuel. Also increasing demand for
49 the alternative fuel due to the fast depleting petroleum diesel has led to biofuel production from
50 vegetable oils. Due to higher cost of edible vegetable oils, production of biofuels from non-edible
51 vegetable oils is preferred [1]. Nowadays, there is very less research on utilizing the non-edible
52 vegetable oils commercially to substitute for petroleum diesel. In this research, esterified waste
53 cooking oil possessing fuel properties on a par with diesel is used as an alternative for diesel [2].
54 Due to chemical structure and dense molar mass, viscosity of WCO is greater in comparison with
55 diesel. This is the major factor which restricts the usage of WCO directly diesel engines [3]. Because
56 of increased WCO viscosity, atomization of fuel and characteristics of spray are greatly affected by
57 the increase in the size of the fuel droplets, thereby lowering the performance and increasing the
58 toxic gas emissions [4]. Viscosity of the WCO oil can be reduced by using various chemical
59 pretreatment methods in which transesterification is one of the most common methods used
60 worldwide [5].

61 Mohamed Al-Dawody obtained biofuel from rapeseed oil and blended it with diesel. He found
62 93.36%, 82.56 %, 81.06%, and 47.27% reduction in smoke emission obtained with B100, B50, B20,
63 and B10 respectively in comparison with diesel. B10 blend emitted less CO and HC with increased
64 NOx [6]. Because of its higher viscosity, there is a decrease in brake thermal efficiency (BTE) with an
65 increase in brake specific fuel consumption (BSFC). Most of the WCO blends emitted higher NOx
66 and lesser CO and HC emissions [7]. Karavalakis et al., [8] studied the effects of WCO biofuel, olive
67 oil, soybean oil and animal fat oil blended with diesel. They concluded that WCO usage increased

68 polyaromatic hydro carbon emissions in the engine due to the presence of cyclic acids and
69 polymerization reaction. Cheung et al., [9] made a detailed study on the WCO biofuel and methanol
70 blends and reported that the increase in aldehyde emissions with lesser alkene emissions. Many
71 researchers [10-12] have used various WCO biofuel-diesel blends in diesel engines and selected B20
72 as the optimal fuel blend. This made the researchers raise the usage of B20 in CI engines. But, due
73 to the increase in NO_x emissions, many researchers [13-15] promoted the usage of alcohols in CI
74 engines because of its lower viscosity and density in comparison with diesel. We could see the
75 usage of various alternative fuels like animal fat oil, soybean oil, rape seed oil, olive oil and WCO in
76 CI engine which reduced various emissions like CO, HC, and smoke with respect to drastic rise in
77 NO_x emission. Wei et al., [16] reported HC, CO, NO_x, and smoke characterisation of a CI engine
78 using WCO biofuel / diesel blends. The outcomes of their research depicted that xylene and toluene
79 were reduced and a decrease in mass concentration of particles was observed. Araujo et al., [17]
80 showed that 45% of production cost could be saved by the usage of WCO biofuel. Due to this usage
81 of WCO biofuel has been increasingly investigated with respect to diesel engines. Di et al., [18]
82 reported various emissions on 4 cylinder CI engine using WCO biofuel with various blends such as
83 100%, 80%, 60%, 40%, and 20% vol respectively at various engine loads. There was a reduction in
84 aldehyde emissions while there was an increase in the formation of benzene and acetaldehyde
85 respectively. Also, similar results were found by Cheung et al., [19] who made investigation using a
86 neat WCO biofuel on 4 cylinder CI engine at different load conditions. The researchers here have
87 discussed the various unregulated emissions from CI engine along with the most needed regulated
88 emissions.

89 From the literature, we could find that the major amount of emission from diesel engine is NO_x
90 which is composed of NO₂ and NO (Nitrogen dioxide and nitric oxide). The former is considered as

91 more toxic than the latter. Formation of NO is one of the main reasons for the depletion of ozone
92 layer and also the formation of smog in the environment which affect the human health. NO is
93 formed inside the cylinder at high temperature zone during diffusion combustion phase. The basic
94 reactions in zeldovich mechanism which determines the decomposition of NOx inside the cylinder
95 are as follows:



99 NOx formation is mainly attributed to oxygen availability and formation of peak temperature
100 inside the combustion chamber. There are various NOx controlling strategies like addition of cetane
101 enhancers, retardation of fuel injection, water injection and exhaust gas recirculation. Cetane
102 enhancers are more expensive while it reports only less amount of NOx reduction. Fuel retardation
103 results in less power with increased SFC, smoke, and HC emissions. Injection of water becomes
104 failure during colder climates and water storage tank is necessary to store the water which would
105 add more weight to the existing engine.

106 EGR is a post treatment method in which exhaust gases are sent to the inlet to replace the
107 fresh air entering into the cylinder. Due to the replacement, oxygen concentration in the fresh air
108 would be reduced. The specific heat of the inlet mixture is increased by the mixing of exhaust gas
109 affecting the fuel-air mixture and ultimately reducing the combustion temperature. Because of this
110 reason, formation of NOx would be greatly reduced. The percentage of EGR can be calculated using
111 the measurement of the concentration of CO₂ at the inlet and the outlet represented as [CO₂]_{int} &
112 [CO₂]_{out} respectively [44].

$$EGR\% = \frac{[CO_2]_{int} - [CO_2]_{atm}}{[CO_2]_{out} - [CO_2]_{atm}} \quad (4)$$

113

114 The percentage of EGR can also be found using the ratio of recirculated exhaust gas mass (M_{EGR}) to
 115 the mass of inlet charge (M_i).

$$EGR\% = \frac{M_{EGR}}{M_i} * 100 \quad (5)$$

116

117 Rajesh Kumar et al., [20] reported that because of oxygen availability in biofuels, there was
 118 reduction in UBHC, CO, and smoke emissions. But NOx emissions were high because of high
 119 temperature of flame. Usage of EGR reduced NOx emissions. Increasing the percentage of EGR in
 120 the inlet air reduced the duration of combustion in the premixed stage and increased the diffusion
 121 combustion stage. It also resulted in ignition delay to be longer [21]. Oxygen concentration at the
 122 inlet was reduced due to the addition of exhaust gas which resulted in the reduction of peak
 123 temperature of combustion. The main reason behind this was the slower reaction rate of
 124 combustion [22]. Though EGR reduced NOx emissions, it increased HC, CO, and smoke emissions.
 125 The rise in HC and CO emissions would be slighter while the increase in smoke emission was
 126 noticeable [23]. Increase in EGR lowered the air-fuel ratio, thereby decreasing the oxygen
 127 availability. This variation in air-fuel ratio increased the various exhaust gas emissions. EGR also
 128 reduced the flame temperature [24]. Das et al., [25] reported on the usage of EGR in a multi
 129 cylinder SI engine along with hydrogen as a pilot fuel and found reduced BSFC and also reduction in
 130 NOx emissions. Because of usage of EGR, the volume of exhaust gases emitted was reduced. Kusaka
 131 et al., [26] also showed that there would be an increase in BTE with reduction in HC emissions when
 132 the inlet air was heated along with EGR at lower load conditions. Increase in UBHC emissions

133 reported around 20-30% was on a par with CI engine with no EGR. Agarwal D et al., also reported
 134 on the increase in HC and reduction in soot emissions in the case of CI engines [27].

135

Table 1 EGR effects on characterisation of diesel and biofuels

Fuel used	EGR Concentration	Engine Specification	Performance	Combustion	Emission	Optimum Fuel and % EGR	Reference
Pentanol / diesel blends, PEN10, PEN20, PEN30, PEN45	10% 20% 30%	Kirloskar TAFE make, DI, 4S, RO - 4.7 kW @ 1500 rpm, IP - 20-21 MPa, IT - 23° bTDC	BTE ▼ BSFC ▲	-	NOx ▼ Smoke ▼ HC ▲ CO ▲	PEN45 20% EGR	[20]
Diesel	10% 15% 20%	Indec PH2, DI, 4S, RO - 9 kW @ 1500 rpm, IP - 210 bar, CR 16.5:1	BTE ▲ BSFC ▼	-	NOx ▼ Smoke ▲ HC ▲ CO ▲	Diesel 15% EGR	[27]
Diesel	2.5% 5% 7.5% 10%	MWM D229-4, DI, 4S, RO - 40 kW @ 1800 rpm, CR - 17:1	BTE ▼ BSFC ▲	HRR ▼ CP ▼	CO2 ▲ CO ▲ HC ▲ NOx ▼	Diesel 7.5 % EGR	[37]

136 PET - Pentanol fuel, IT - Injection timing, RO - Rated Output, CR - Compression ratio, 4S - Four
137 Stroke, IP - Injection Pressure.

138 Most fluid flow problems can be solved using Computational Fluid Dynamics (CFD) software. By
139 defining the boundary conditions, various CFD software like ANSYS Fluent could perform
140 simulations of the fluid interactions. Furthermore, to make a good research, before conducting the
141 experiments, it is better to get solutions by simulation. Rajesh Govindam et al. [28] prepared
142 different models to analyse various blends of biofuel in the diesel engine using ANSYS Fluent. High
143 peak temperature and in-cylinder pressure were obtained as results while validating the models.
144 Norrizam Jaat et al., [29] predicted the characteristics of combustion with high peak pressure and
145 temperature with ambient conditions for Jatropha biofuel in diesel engine using Ansys Fluent. The
146 usage of simulation software has improved the confidence in conducting the experiments and
147 would easily make the comparison in the obtained results.

148 M.S.Gad et al [45] conducted experiments on the diesel engine with WCO biodiesel and
149 gasoline additives to compare the performance, emission and combustion characteristics with neat
150 diesel fuel. Three fuel blends namely BG8, BG4, and BG2 consisting of 8%, 4%, and 2% gasoline and
151 92%, 96%, and 98% WCO respectively were used. The emissions such as smoke, NO_x, HC and CO
152 were reduced by 30%, 20%, 30%, and 25% respectively along with improved cylinder pressure and
153 heat release rate due to the usage of WCO and gasoline additives. Mohamed Nour et al [46]
154 investigated the aluminium oxide nano particle addition over the ethanol blended jojoba biodiesel
155 in a diesel engine and found that 75 mg/L addition of nano particle enhanced the overall
156 characteristics of the engine. Ahmed I. El-Seesy et al [47] conducted an experimental investigation
157 in the diesel engine to optimize the aluminium oxide nanoparticle addition over jojoba biodiesel
158 blends. They found that 20 mg/L of nanoparticle addition reduced the emissions such as smoke, HC,

159 CO and NO_x by 35%, 60%, 80%, and 70% respectively. While 40 mg/L addition showed remarkable
160 improvement in performance and combustion characteristics of the engine.

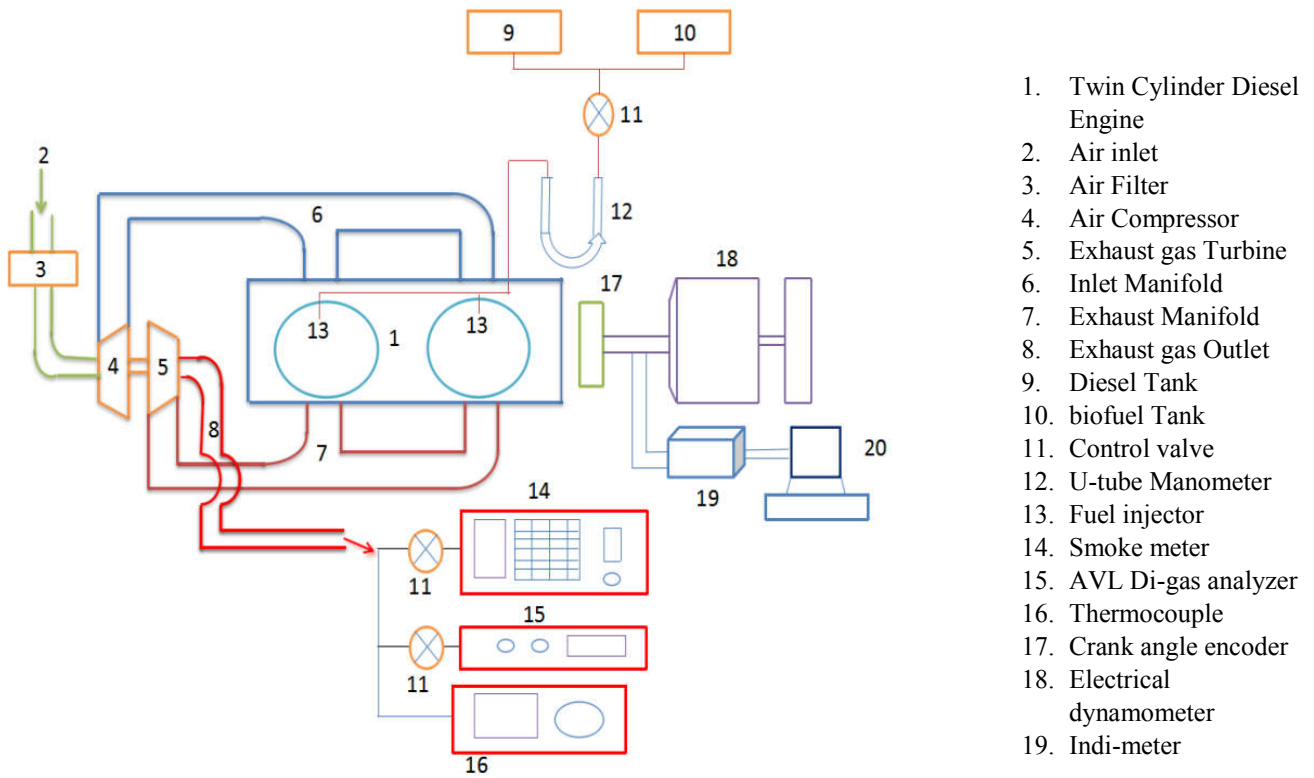
161 From the literature, it is clear that WCO biofuel can be used as an alternative fuel in CI engines
162 along with reduction in various emissions like CO, HC, and smoke along with increased NO_x. To
163 control NO_x emission, EGR was found to be an effective method. Many researchers made efforts to
164 optimize the WCO fuel blend which ended in increasing NO_x. Only very less number of research
165 works was found in the area of optimizing the WCO fuel blend along with reduction in NO_x and
166 without compensating the performance and other emissions. Thus, in this research work, WCO
167 biofuel is prepared using transesterification method and it is analyzed using gas
168 chromatography-mass spectroscopy (GCMS) method. It is then mixed with diesel in vol proportions
169 such as 100%, 60%, 40%, and 20% respectively. The fuel properties of the prepared blends were
170 studied. The combustion modeling has been done for the prepared blends of biofuel, B100, and
171 diesel which are compared by using ANSYS Fluent software. Also characterisation on combustion,
172 performance, noise and emission of various test fuels has been studied in a two cylinder CI engine.
173 Depending upon experimental characterisation and simulated results of combustion, a suitable
174 blend ratio is selected for the WCO biofuel. Further to reduce NO_x emissions in the selected blend
175 ratio, EGR is introduced into the inlet at varying ratio of 5%, 10%, and 15% respectively. Thus
176 optimization has been done in terms of percentage of EGR introduced in the optimized WCO blend.

177 **2. Materials and Methods**

178 **2.1 Test Engine Set-up**

179 A twin cylinder, water cooled, 4 stroke, D.I diesel engine was used for the current investigation.
180 The complete schematic representation of the test engine setup with EGR used is in fig. 1. Fig. 2
181 shows the actual engine set-up. This type of engine is used in the case of tractors falling under

182 Bharat Stage-III norms. The major engine specifications are listed in Table 2. The various
 183 instruments used for the characterisation of the test engine and uncertainties and errors predicted
 184 using a separate method in the experimental calculations [30] are detailed in Table 3.



185

186

Fig. 1 Schematic diagram of engine setup using EGR



187

188

Fig. 2 Engine Setup

189

Table 2 Engine Specifications

Parameter	Specification
Model and make	Simpons S217 Tractor Engine
Maximum Rating	21 kW @ 2000 rpm
Cubic Capacity	1670 cc
Configuration type	Vertical In-Line Diesel Engine
Injection system	Direct Injection
Bore	91.44 mm
Stroke	127 mm

Compression Ratio	18:5:1
Connecting rod length	223.81 mm
No of Cylinders	Two
Aspiration	Natural
Cycle	4 Stroke
Cooling System	Water cooled
Governing	Mechanical
Fuel Pump	Mico Bosch In-line Pump
Injection Timing	24° bTDC
Lubricating Oil	SAE 1 or SAE 3
No. of nozzle holes	5
Injector nozzle size	0.262 mm @ 148°
Injection Pressure	250 bar

190

191

Table 3 Measuring Instruments used

Instruments used with model	Measuring parameter	Measuring range	Accuracy	Errors
E50 Eddy Current	Torque	234 Nm @ 1500 to 3000 rpm	± 0.25	± 0.2

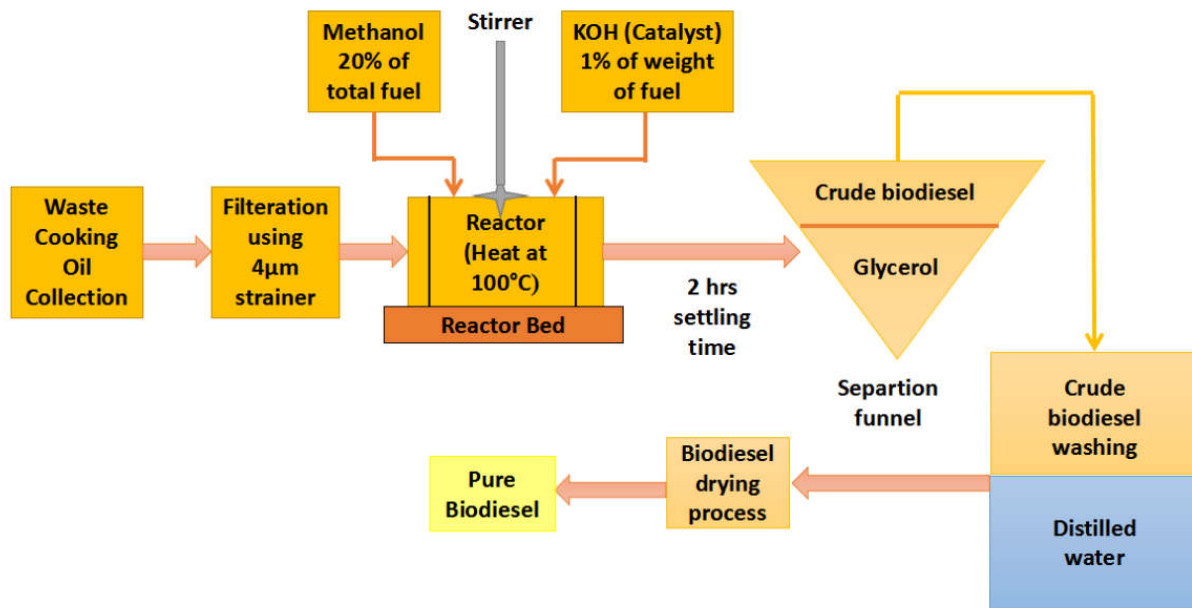
Dynamometer				
FMGDN80G100 Air flow meter	Amount of flow of air	160 m ³ /hr	± 1	± 1
6613CQ09-01 KISTLER Pressure Sensor	Pressure	0 - 200 bar	± 0.75	± 0.1
AVL DI GAS 444N analyser	CO	0 – 15 % vol	± 0.013	± 0.9
	HC	0 – 20,000 ppm	± 3	± 1.1
	O ₂	0 – 25 % vol	± 0.025	± 0.8
	CO ₂	0 – 20 % vol	± 0.1	± 1.05
	NO _x	0 – 2,000 ppm	± 5	± 1.15
AVL 437 smoke-meter	Smoke	0 - 100% capacity	± 1	± 1

192

193 2.2 Biofuel preparation

194 In this research work, Waste Cooking Oil (WCO) was collected from the hostel mess of Mepco
195 Engineering College, Sivakasi. The oil was used to fry papads served during lunch. A one step
196 transesterification process shown in fig. 3 was done to convert the raw WCO into biofuel. In this
197 process, solid filtration was done by using a strainer of 4µm in which the filtered oil was then
198 heated to about 100°C for around 15 minutes. The heating was done to eliminate water particles
199 present in the WCO oil. Using a mechanical stirrer, constant stirring at 1000 rpm for 10 minutes is
200 done by adding 1% weight of potassium hydroxide and methanol to the heated oil. The
201 ultrasonicator bath was kept constant at 65°C. The mixture obtained was allowed to settle down for

202 2 hours in a separation vessel. Three different blends, namely B20, B40 and B60 were prepared
 203 respectively. Analysis was made on all the three prepared blends & WCO and compared with
 204 respect to diesel. The physio-chemical properties of the fuel estimated using different methods of
 205 standard are listed in Table 4.



206

207

Fig. 3 Biofuel Production

208

Table 4 Determination of test fuel properties

S.No	Fuel properties	Diesel	B20	B40	B60	B100	ASTM Test standard
1	Kinematic Viscosity @	2.31	2.04	2.77	3.23	4.07	D445

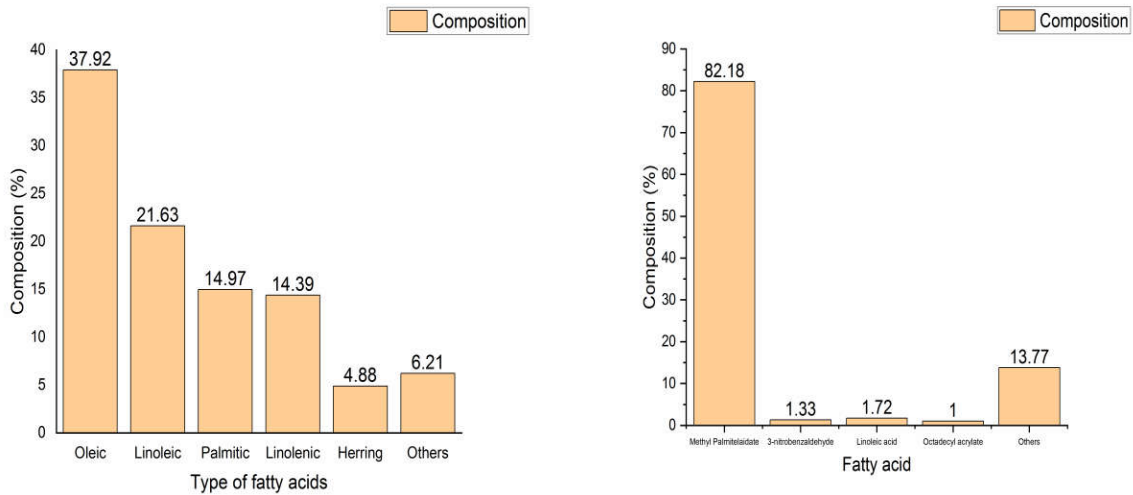
	40°C (cSt)						
2	Density (kg/m ³)	832	820	837	853	875	D4052
3	Calorific Value (kJ/kg)	42485	41448	40091	38452	36123	D240
4	Flash point (°C)	71	88	127	163	186	D93

209

210 **2.3 GCMS results of waste cooking oil and biofuel**

211 The GCMS technique was employed to find out the chemical constituents that were present in
 212 the fuel. This is a type of analytical method to differentiate substances in a test fuel using gas
 213 chromatography and mass spectrometer. Fig. 4(a) represents the fatty acid contents of WCO and fig.
 214 4(b) shows the methyl ester compounds that are present in WCO biofuel.

215



216 **Fig. 4 Bar chart of (a) % Fatty acid present in WCO and (b) % methyl ester compounds present in**
 217 **the WCO biofuel**

218 The GCMS results obtained for WCO are presented in Table 5. The major constituent
 219 chemicals which are present in WCO consist of 37.92% of fatty acid type of oleic acid. The second
 220 major constituent of around 21.63% of fatty acid type is linoleic acid. The third and the fourth fatty
 221 acid contents present are 14.97% of palmitic acid and 14.39% of linolenic acid respectively. WCO
 222 had 264 g/mol as average molecular weight. The GCMS results of WCO biofuel are presented in
 223 Table 6. About 82.18% of the WCO biofuel obtained had methyl ester palmitate. 1% of octadecyl
 224 acrylate, 1.72% of linoleic acid and 1.33% of 3-nitrobenzaldehyde are the other minor chemical
 225 constituents that are present in the WCO biofuel. The author has given a more detailed description
 226 in his previous study [41] about the GCMS of WCO and WCO biofuel and so it is not explained now
 227 in a detailed manner.

228 **Table 5 Fatty acid composition of waste cooking oil**

S.No	Peak no	Identified compounds	Molecular Weight	Molecular formula	Area

1.	14	Cyclopentadecanone, 2-hydroxy-	240.3816	C ₁₅ H ₂₈ O ₂	15.79
2.	5	13-octadecadienol, Z-3, 2-Methyl-Z	280.548	C ₁₉ H ₃₆ O	12.17
3.	1	n-hexadecanoic acid	256.43	C ₁₆ H ₃₂ O ₂	9.04
4.	4	trans-13-Octadecenoic acid	282.468	C ₁₈ H ₃₄ O ₂	7.37
5.	16	Oleic Acid	282.468	C ₁₈ H ₃₄ O ₂	7.23
6.	12	2-Oxecanone, 10-methyl-,	170.2487	C ₁₀ H ₁₈ O ₂	4.6
7.	22	2-Trifluoromethylbenzoic acid, 1-cyclopentylethyl ester	190.121	C ₈ H ₅ F ₃ O ₂	4.46
8.	20	2-Trifluoromethylbenzoic acid, 1-cyclopentylethyl ester	190.121	C ₈ H ₅ F ₃ O ₂	4.19
9.	11	Oleic Acid	282.468	C ₁₈ H ₃₄ O ₂	3.46
10.	2	Octasiloxane, 1,1,3,3,5,5,7,7,9	577.233	C ₁₈ H ₅₄ O ₇ Si ₈	3.07
11.		Octasiloxane, 1,1,3,3,5,5,7,7,10		C ₁₆ H ₄₈ O ₇ Si ₈	
12.	15	Oleic Acid	282.468	C ₁₈ H ₃₄ O ₂	2.92
13.	19	2-[(tert-butyl dimethyl silyl)oxy]-1-isopropyl-4-methyl-, Benzene	264.484	C ₁₆ H ₂₈ OSi	2.18
14.	6	Octadec-9-enoic acid	283.46	C ₁₈ H ₃₄ O ₂	1.92
15.	18	N-(1-methylethyl)-N,3-diphenyl-, 2-Propenamide	252.358	C ₁₄ H ₂₄ N ₂ O ₂	1.84
16.	17	6-Octadecenoic acid	282.468	C ₁₈ H ₃₄ O ₂	1.63
17.	21	[4-(1,1-dimethylethyl)phenoxy]-, Acetic acid, methyl ester	222.284	C ₁₃ H ₁₈ O ₃	1.62
18.	8	2-p-Nitrophenyl-5-ethoxy-oxadiazole-1,3,4	70.051	C ₂ H ₂ N ₂ O	1.43
19.	9	2,4-dimethyl, Benzo[h]quinoline	207.276	C ₁₅ H ₁₃ N	1.26

20.	7	2-Ethylacridine	207.276	C ₁₅ H ₁₃ N	1.19
21.	10	n-Decanoic acid	172.268	C ₁₀ H ₂₀ O ₂	1.11
22.	13	6-Octadecenoic acid, (Z)	282.468	C ₁₈ H ₃₄ O ₂	1.08
23.	3	(E,E)-2,4-Decadienal,	152.237	C ₁₀ H ₁₆ O	0.27

229

230

Table 6 FAMES composition of WCO biofuel

S.No	Peak	Identified compounds	Molecular formula	Molecular Weight	Area
1.	3	Methyl ester, 10,13-Octadecadienoic acid	C ₁₉ H ₃₄ O ₂	294.479	53.99
2.	1	Methyl ester, 9-Octadecenoic acid	C ₁₉ H ₃₆ O ₂	296.495	22.49
3.	2	Methyl ester stearic acid	C ₁₉ H ₃₈ O ₂	298.511	4.71
4.	12	Methyl ester, cis-13-Eicosenoic acid	C ₂₁ H ₄₀ O ₂	324.549	0.97
5.	8	cis-13-Octadecenoic acid	C ₁₈ H ₃₄ O ₂	282.468	0.97
6.	11	4-Hydroxybenzoxazolone	C ₇ H ₅ NO ₃	151.121	0.92
7.	4	13.trans.-octadecatrienoate, Methyl 9.cis.,11.trans.t	C ₁₉ H ₃₂ O ₂	292.463	0.89
8.	5	methyl ester, 9-Octadecenoic acid, (E)-	C ₁₉ H ₃₆ O ₂	296.495	0.55
9.	7	9,12-Octadecadienoic acid (Z,Z)-	C ₁₈ H ₃₂ O ₂	280.452	0.55
10.	6	Methyl ester, eicosanoic acid	C ₂₁ H ₄₂ O ₂	326.565	0.4
11.	9	9,12-Octadecadienoic acid (Z,Z)-	C ₁₈ H ₃₂ O ₂	280.452	0.4
12.	10	9-Dicarboxylic acid, Tricyclo[5.2.1.0(2,6)]dec-8-ene-8, 4-methylene-, dimethyl ester, endo	C ₆ H ₁₂ FNO	133.166	0.31

231

2.4 Test Procedure

232

233 The experiments were carried out at 100%, 75%, 50%, 25% load conditions of the engine with
 234 respect to the indicated mean effective pressure of 5.29, 2.73, 1.64, and 1.16 bar respectively. The
 235 lubricating oil was maintained at temperatures between 68 and 88°C. The test engine had 24°
 236 Crank Angle bTDC and the pressure of injection was maintained at 250 bar. Throughout the
 237 experiments, the room temperature was maintained at ambient conditions to increase the
 238 reliability in the readings [49-50]. To start the trial for each run, the engine was allowed to run for
 239 5-10 mins with the respective fuel before the recording of the readings [53-55]. Every test done was
 240 repeated thrice, and the average values were taken for the plotting of the graph, and so
 241 repeatability was ensured [51-52]. Table 7 represents the design matrix of test fuels used along
 242 with their blending percentage and EGR conditions.

243 **Table 7 Summary of test fuels, blends & conditions**

Fuel No.	Test Fuel								EGR condition			Short form of fuel
	Diesel, vol%				WCO				5 %	10 %	15 %	
	100 %	80 %	60 %	40 %	20 %	40 %	60 %	100 %				
1	√											D100
2		√			√							B20
3			√			√						B40
4				√			√					B60
5								√				B100
6		√			√				√			B20 5%EGR
7		√			√					√		B20 10%EGR
8		√			√						√	B20 15%EGR

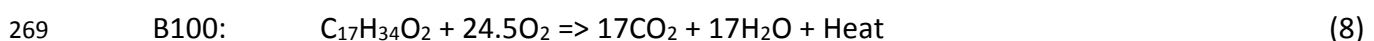
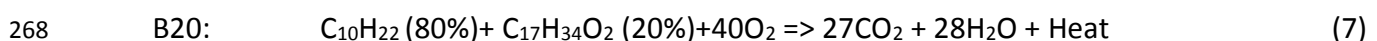
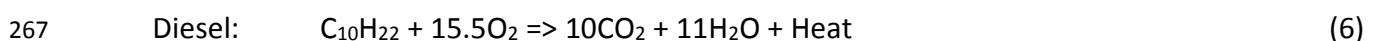
244

245 3. CFD analysis of fuel combustion using Ansys Fluent

246 3.1 Problem Modeling

247 A cylindrical combustion geometry of dimensions 1800 mm * 225 mm was created by using
248 Ansys Modeller. The geometry was meshed using Ansys represented in fig 5 and the edges were
249 named as per the requirements for applying boundary conditions.

250 The properties of the fuel were taken from table 5 for combustion analysis. Turbulence
251 Chemistry Interaction-Eddy Dissipation model was used in the analysis of combustion of biofuel to
252 assume it as a complete combustion. The combustion modeling for three different fuels namely,
253 diesel, B20, and B100 was carried out. The type of analysis used was 2D axisymmetric. K-epsilon
254 type of turbulence model was implemented. The simulation was made to run initially on the
255 created mesh and ensured the predicted results of temperature, NOx and CO₂ were steady and also
256 the imbalances accuring below 1% along with 10⁻⁴ residual error. Again the simulation was made to
257 run with another mesh which was finer about 1.5 times the size of the intial element mesh. Now
258 the imbalances were below 1%, residual error dropped below 10⁻⁴ and the predicted results of
259 temperature, NOx and CO₂ were steady. The difference in the points which was monitored
260 between the two simulations were within the acceptable limits. Again the mesh element size was
261 reduced and the points mointored were found steady. The number of iterations were around 6
262 with different element sizes varying from 13 mm - 0.7 mm respectively. As finer the mesh
263 resolution, the results were accurate. While 12000 number of elements with element size of about
264 1 mm has been found better with respect to the accuracy in results and also with the simulation
265 runtime. Thus the solution predicted was found independent of the mesh that has been created
266 [48]. The basic combustion equations for various elements are:



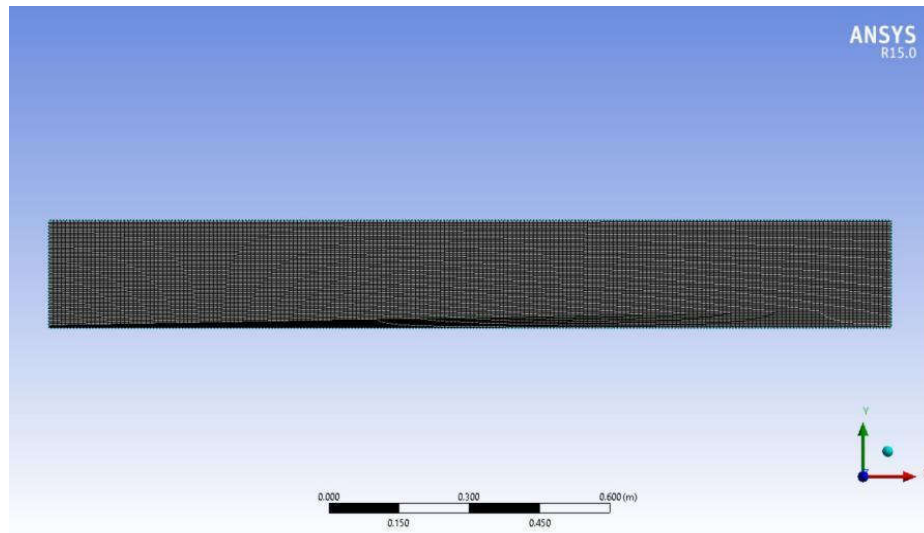
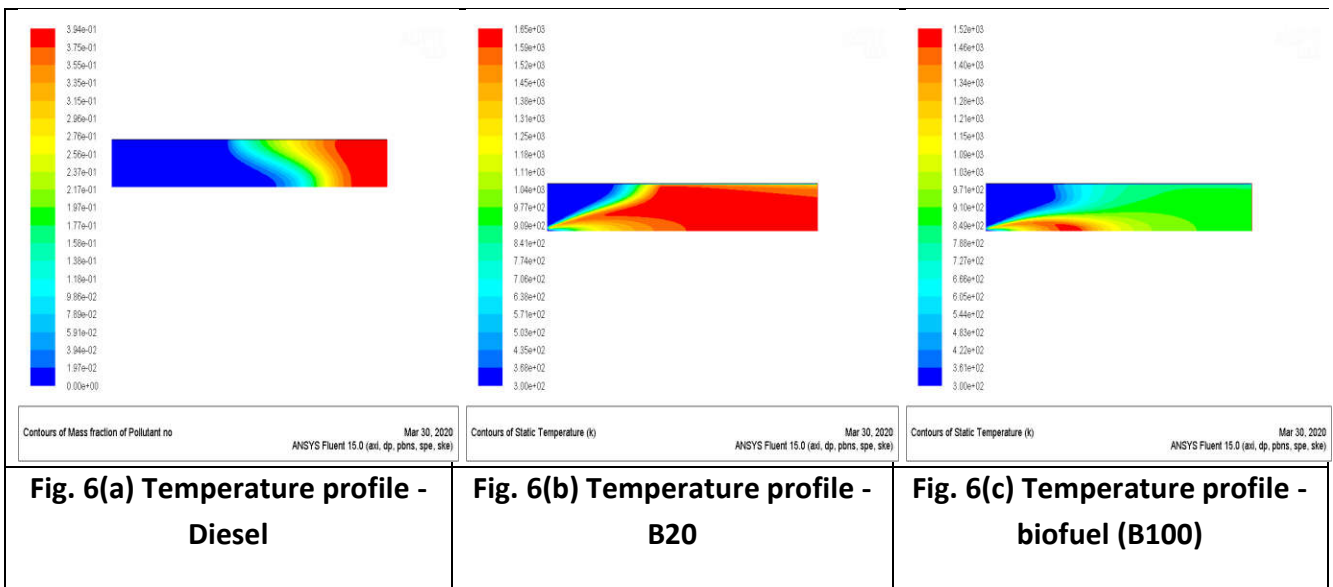


Fig. 5 Meshed cylindrical combustor

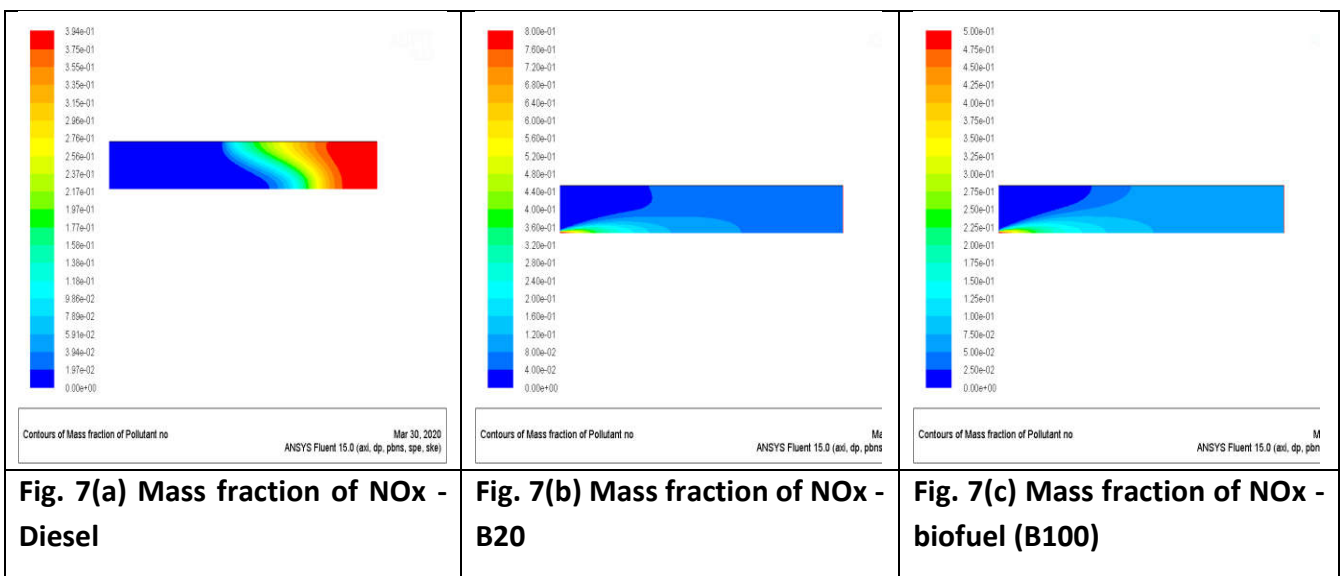
3.2 Predicted Results:

The mass fraction of O_2 was 0.76 at 0.5m/s,300K at the air inlet and the mass fraction of diesel/biofuel at the fuel inlet was 1 at 50m/s,300K. The major properties of diesel considered were viscosity as 2.76 cSt, calorific value as 44000 kJ/kg, density as 825kg/m³, and specific heat constant as 1750 J/kg-K. The temperature profile of diesel-air mixture shown in fig 6(a) was predicted with a peak temperature of about $2.12e^{+03}$ K. The high temperature was because of high heating value and low viscosity of diesel. The major properties of B20 considered were viscosity as 2.93 cSt, calorific value as 41417.42 kJ/kg, density as 820kg/m³, and specific heat constant as 2050 J/kg-K. The temperature profile of biofuel (B20) - air mixture shown in fig 6(b) was predicted with a peak temperature of about $1.652e^{+03}$ K. The low temperature in comparison with diesel was because of low heating value and increased viscosity of B20 blend. The major properties of biofuel (B100) considered were viscosity as 4.07 cSt, calorific value as 36099.34 kJ/kg, density as 875kg/m³, and specific heat constant as 2050 J/kg-K. The temperature profile of biofuel (B100) - air mixture shown in fig 9(c) was predicted with a peak temperature of about $1.52e+03$ K which was lesser than the conventional diesel-air mixture. The reason would be the same as mentioned for B20 blend.

287 The contours of mass fraction of pollutant NOx emission of diesel are depicted in fig 7(a)
 288 ranging between 0.12 and 0.39 mass fraction. The contours of mass fraction of pollutant NOx
 289 emission of B100 fuel are shown in fig 7(c) ranging between 0.1 and 0.5 mass fraction. The contours
 290 of mass fraction of pollutant NOx emission of B20 fuel are shown in fig 7(b) ranging between 0.12
 291 and 0.8 mass fraction. The mass fraction of NOx produced was higher in B20 than in B100 and
 292 diesel fuel during combustion. This increase in mass fraction of NOx could be reduced by the
 293 application of EGR introduced into the inlet air.

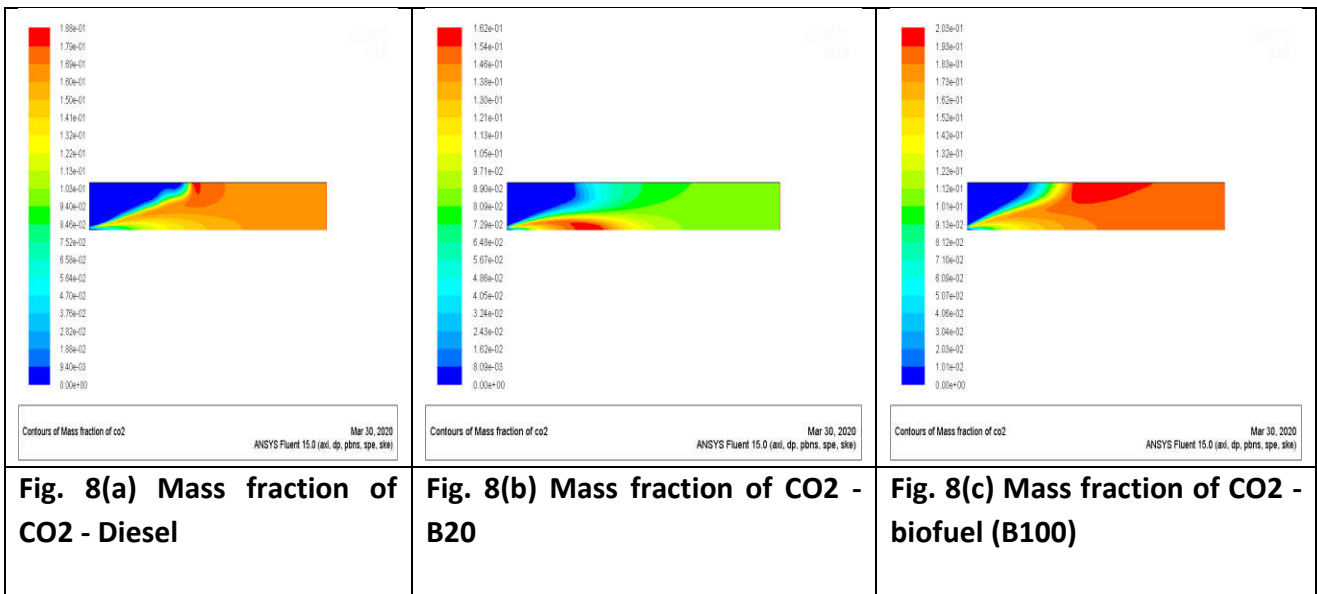


294



295

296 The contour of mass fraction of CO₂ emission of diesel is shown in fig 8(a) ranging between 0.1
 297 and 0.19 mass fraction. The contour of mass fraction of CO₂ emission of biofuel (B100) are shown in
 298 fig 8(c) ranging between 0.1 and 0.2 mass fraction. The contour of mass fraction of CO₂ emission of
 299 biofuel (B20) are shown in fig 8(b) ranging between 0.1 and 0.16 mass fraction. In comparison with
 300 all the three CO₂ emission mass fractions, B20 fuel seems to perform better with which there are
 301 no differences in the case of B100 and diesel fuel.



302

303 4. Results and Discussions

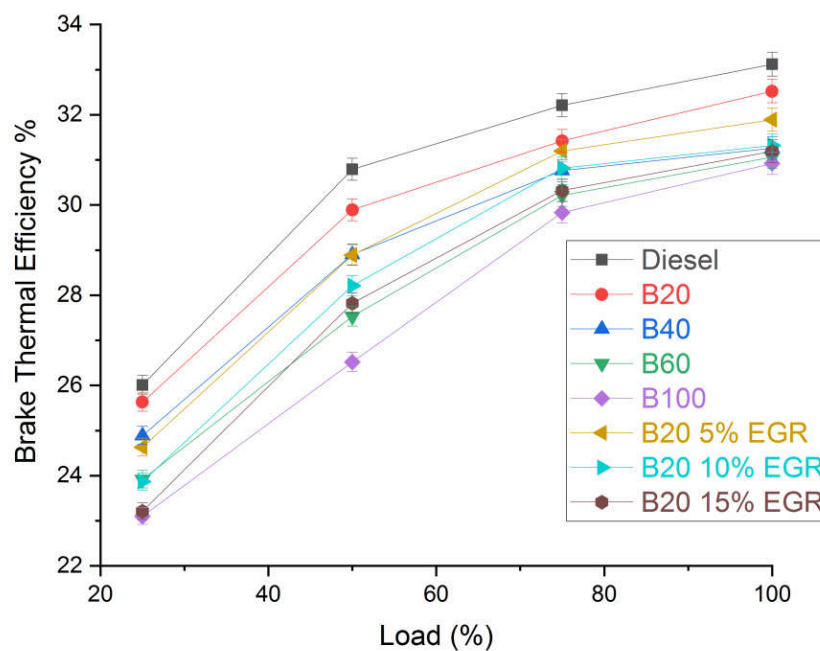
304 4.1 Characteristics of Performance

305 4.1.1 Variation in BTE

306 Fig. 9 represents comparison of BTE of diesel, WCO biofuel and prepared blends with increase
 307 in load. The graph explains clearly about the conversion of heat into work. BTE was calculated using
 308 engine torque, speed, and rate of fuel consumption. The graph shows a general trend done by
 309 various researchers [35, 36] in which BTE increases with rise in load for all types of test fuels. The
 310 upper limits of BTE obtained at 100% load condition are 33.12, 30.92, 31.06, 31.26, and 32.52

311 percentage for diesel, B100, B60, B40, and B20 respectively. Increasing blend percentage of WCO
312 biofuel in diesel decreased BTE. The main reason behind this trend was increasing viscosity and
313 decreasing calorific value with respect to the increase in blending percentage of biofuel. B20 blend
314 fuel behaved very much like pure diesel and better than other blends of WCO biofuel [34].

315 In the view of controlling NO_x in the B20 blend fuel, exhaust gases were introduced into the air
316 inlet at 5, 10, and 15 % respectively. From fig. 9, percentage increase in EGR would slightly decrease
317 BTE. The main reason was reduction in the rate of burning impinging the normal combustion
318 process of B20 fuel blend. The combustion losses were increasing due to increase in EGR rates.



319

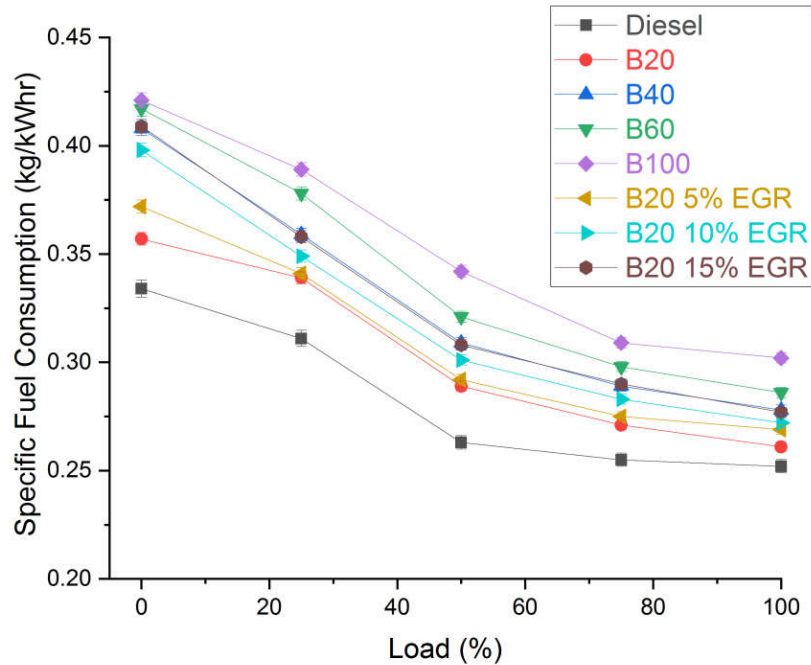
320

Fig. 9 Load Vs Brake Thermal Efficiency

321 4.1.2 Variation in SFC

322 Fig. 10 represents comparison of SFC of diesel, WCO biofuel and its blends with increase in
323 load. The graph shows a general trend observed by various researchers [33, 35] in which SFC fell

324 with rise in load for all types of test fuels. The SFC measured at 25% load condition were 0.311,
 325 0.389, 0.378, 0.359, and 0.339 kg/kWhr for diesel, B100, B60, B40, and B20 respectively.
 326 Comparison shows the increase in SFC at all load conditions with the increasing percentage of
 327 biofuel blends. Biofuel has extracted the same power output with more consumption of fuel in
 328 comparison with diesel due to high density and lower calorific value. The difference between SFC at
 329 lower loads was high while at higher load conditions it was found to be low. Since at higher loads,
 330 the air fuel mixture inducted into the cylinder became lean which consumed lesser amount of fuel.
 331 From fig. 10, increasing rates of EGR would slightly increase SFC at lower loads, while at higher
 332 loads no much difference was found [20]. The reason at high loads was that the mixture was
 333 becoming lean, while at lower loads in-cylinder temperature decreased causing incomplete
 334 combustion due to increase in EGR application.



335
 336 **Fig. 10 Load Vs Specific Fuel Consumption**

337 **4.2 Characteristics of Various Emissions**

338 4.2.1 Variation in CO emission

339 Fig. 11 depicts the comparison of CO emission values of diesel, WCO biofuel and prepared
340 blends along with increase in load. The graph shows a general trend seen by a researcher [33] in
341 which CO emission increases sharply for higher load for all types of blends and fuels including both
342 diesel and WCO biofuel. This rise is because of increased fuel injection inside the combustion
343 chamber and very less time for the combustion to take place. At lower and medium load conditions,
344 only slight differences are observed in CO emissions for the blends. But still, with the increase in the
345 blending percentage of WCO, CO emission decreases. This is due to plenty of oxygen available in
346 WCO biofuel resulting in CO₂ conversion at lower and medium loads [35]. At 100% load condition,
347 CO emissions obtained are 0.1, 0.09, 0.09, 0.08, and 0.07 % vol for diesel, B100, B60, B40, and B20
348 respectively. B20 blend serves better in comparison with other higher blends. This is due to less
349 time for combustion into which increased availability of oxygen in increasing WCO blends quenches
350 the flame and reduces the flame temperature. Increase in variation of EGR rates in B20 fuel
351 increases CO emission since EGR introduction reduces the oxidation reaction of CO to CO₂ by
352 decreasing the available oxygen level and replacing it by CO₂ at the inlet.

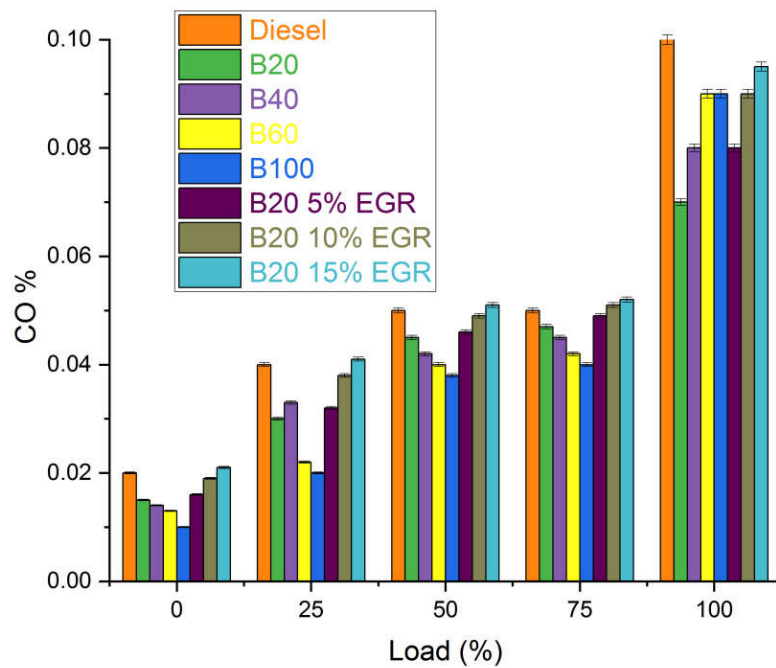


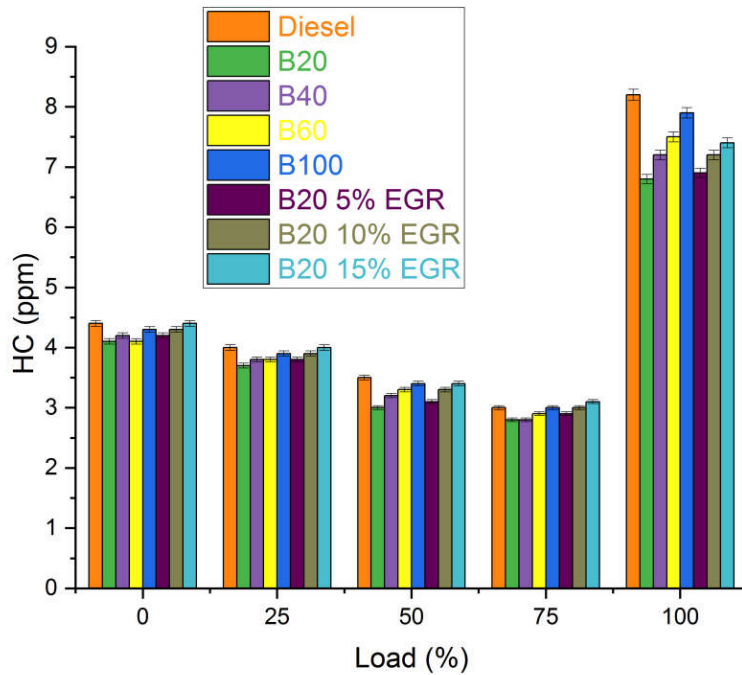
Fig. 11 Load Vs CO Emission

4.2.2 Variation in HC Emission

Fig. 12 represents the comparison of HC emission values of diesel, WCO biofuel and its prepared blends with respect to change in load. The graph shows a trend in which HC emission decreases for lower and medium loads for all types of blends and fuels including both diesel and WCO biofuel. At 100% load condition, HC emissions obtained are 8.2, 7.9, 7.5, 7.2, and 6.8 for diesel, B100, B60, B40, and B20 respectively and they are increasing for all types of fuels [33]. Increased mass of fuel inducted to produce engine power leading to incomplete combustion would be a major reason. Increasing the blend percentage of WCO at lower and medium load conditions does not have a major effect in HC emission between the blends but still less than diesel fuel. The reason could be that increased oxygen level in WCO biofuel facilitates complete burning inside the combustion chamber. At higher loads, B20 has performed better than all other blends. Here the reason could be the presence of lean air fuel mixture getting quenched due to excess oxygen

367 available in WCO biofuel guiding to incomplete combustion. Increasing percentage of EGR in B20
 368 blend increases HC emission [27] since the rise in EGR rates produces larger zones of flame
 369 quenching at the diffusion stage of combustion.

370



371

372

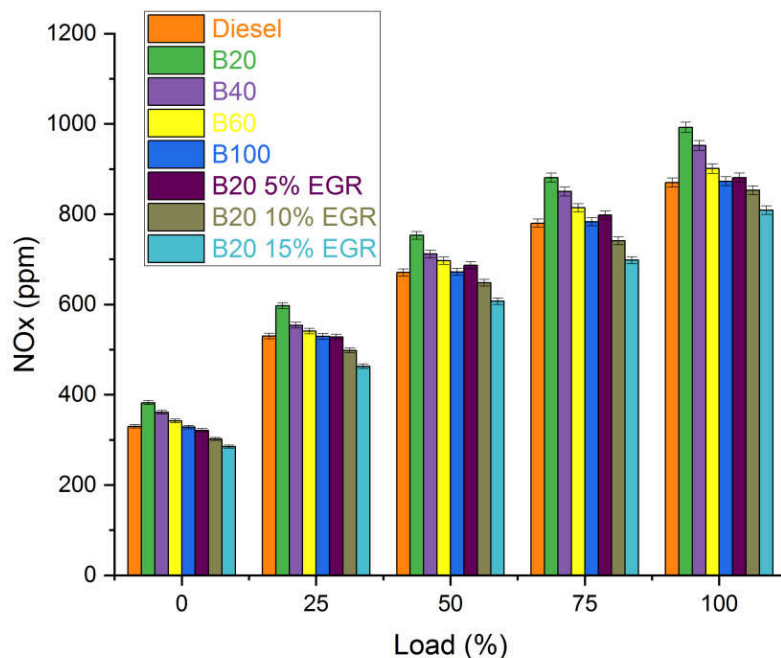
Fig. 12 Load Vs HC Emission

373

4.2.3 Variation in NOx Emission

374 Fig. 13 shows the trade-off between NOx emission values of diesel, WCO biofuel and its
 375 prepared blends with respect to change in load. The graph shows a general trend noted by various
 376 researchers [6, 7, 16] in which NOx emission increases with respect to rise in load for all types of
 377 test fuels. The reason is rise in flame temperature due to quick reaction rate with increase in load
 378 [34]. Increased oxygen level in biofuel enables complete burning thus increasing in-cylinder
 379 temperature and also due to high heat release rate NOx emission increases. The trends between

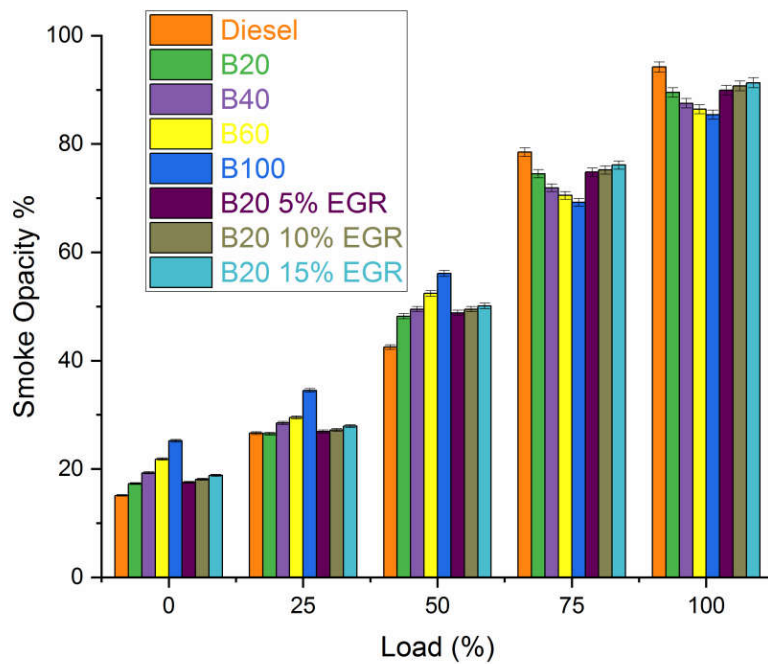
380 the blends are the same at all load conditions. At 100% load condition, NOx emissions obtained are
 381 870, 873, 901, 952, and 992 ppm for diesel, B100, B60, B40, and B20 respectively. From the above
 382 values, all WCO blends and biofuel have higher NOx than diesel. This would be ascribable to better
 383 burning at diffusion phase and biofuel accumulation at the premixed phase of combustion. B20
 384 shows higher NOx emission compared with other blends and biofuel. The reason is higher
 385 cumulative heat release rate rendered by oxygen content to the diesel to burn effectively and
 386 produce higher flame temperature. To reduce NOx emission in B20 blend fuel, EGR is introduced
 387 into the inlet. With the increase in percentage of EGR, NOx emission decreases. Exhaust gases
 388 reduce the oxygen level in the combustion by replacing it with CO₂. The reduction in NOx is higher
 389 at full load while it is lower at part loads. The reason is that oxygen availability for combustion
 390 decreases as the load increases, thus reducing the cylinder flame temperature.



391
 392 **Fig. 13 Load Vs NOx Emission**

393 **4.2.4 Variation in Smoke Emission**

394 Fig. 14 depicts the trade-off between smoke opacity values of diesel, WCO biofuel, and its
395 prepared blends with respect to increase in load. The graph shows a trend observed by various
396 researchers [6, 7, 16] in which it shows an increase in smoke opacity with respect to rise in load for
397 all types of test fuels. This is due to the consumption of increased quantity of fuel and lesser air fuel
398 equivalence ratio at higher loads. At 100% load condition, smoke opacities are 94.2, 85.4, 86.4, 87.5,
399 and 89.5% and at 50% load, smoke opacities are 42.5, 56.1, 52.4, 49.5, and 48.2% for diesel, B100,
400 B60, B40, and B20 respectively. This trend between the blends shows that at lower and part loads,
401 smoke opacity increases with the rise in blends of WCO biofuel. The reason is air fuel mixture being
402 rich, increases the viscosity of WCO biofuel and atomization of fuel being poor. While at higher load
403 conditions, though B100 has high viscosity, air-fuel mixture is lean and so high oxygen content
404 available in biofuel combusts the mixture at a better rate than diesel and other WCO blends. B20
405 fuel has shown a better result for smoke opacity at higher loads and at lower and part loads, there
406 is no much difference from diesel fuel. Increase in percentage of EGR raises smoke opacity with
407 respect to change in load [27]. The reason behind is that the mixing of exhaust gas reduces the
408 oxygen availability leading to incomplete combustion. In general, soot bump occurs with the
409 increase in EGR rates thus making it difficult to control the combustion inside the cylinder.

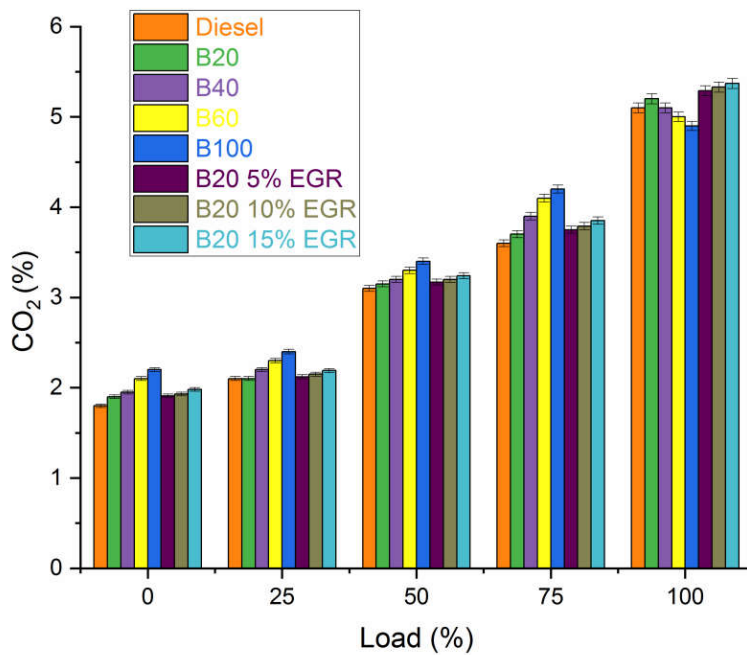


410
411 **Fig. 14 Load Vs Smoke Emission**

412 **4.2.5 Variation in CO₂ Emission**

413 Fig. 15 represents the comparison of CO₂ emission values of diesel, WCO biofuel, and prepared
 414 blends along with increase in load. The graph shows a similar trend noticed by researcher [32] in
 415 which CO₂ emission increases gradually at all load conditions for all types of blends and fuels
 416 including both diesel and WCO biofuel. This rise is due to the increased mass of fuel injection inside
 417 the combustion chamber. With increase in blending percentage of WCO, CO₂ increases. The reason
 418 is plenty of O₂ available in WCO biofuel resulting in CO to CO₂ conversion. At 100% load condition,
 419 CO₂ emission obtained are 5.1, 5.7, 5.5, 5.4, and 5.2 % vol for diesel, B100, B60, B40, and B20
 420 respectively. B20 blend serves better in comparison with the other higher blends only at lower and
 421 part load conditions. The reason is that rich air fuel mixture burning needs more oxygen content
 422 which is less in B20 in comparison with its higher blends. At higher loads, B20 fuel has higher CO₂
 423 emissions than the other blends since less oxygen content in comparison with its higher blends

424 prevents the flame quenching thus increasing the conversion of CO to CO₂. Increase in the
 425 percentage of EGR in B20 blend increases CO₂ emission with the increase in load since EGR
 426 introduction has substantial amount of CO₂ in the exhaust gas which is sent into the fresh air inlet
 427 which contains some negligible amount of CO₂ thus increasing the emission at the outlet [37].
 428



429

430

Fig. 15 Load Vs CO₂ Emission

431

4.2.6 Variation in Exhaust gas temperature

432

433

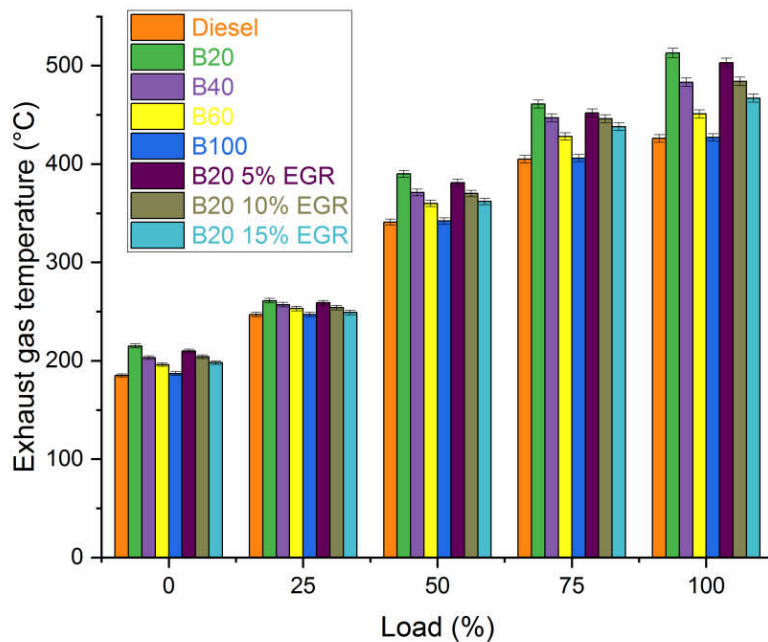
434

435

436

Fig. 16 depicts the trade-off between EGT values of diesel, WCO biofuel, and its blends with the increase in load. The graph shows a similar trend observed by various researchers [32, 35] in which EGT increases along with increase in load conditions for all types of test fuels. The reason behind this was burning of more amount of fuel at higher load and higher engine in-cylinder temperature. On comparing the fuels, WCO blends performed better than diesel. At 100% load condition, EGT

437 values are 426, 427, 451, 483, and 513 °C for diesel, B100, B60, B40, and B20 respectively since
 438 blends had high release rate which helped them in complete combustion increasing EGT. But
 439 increase in percentage of WCO blend has led to a decrease in EGT. This is because of high oxygen
 440 availability and the consequent flame quenching taking place at the diffusion combustion phase.
 441 Increase in the percentage of EGR increases EGT for B20 fuel. The reason might be higher specific
 442 heat of air at inlet [36] and also less oxygen availability at the inlet as discussed in the earlier
 443 sections.



444

445

Fig. 16 Load Vs Exhaust Gas Temperature

446 **4.2.7 Emission variation**

447 The table 8 represents the comparison of various emissions parameters as a summary. The
 448 main aim of this research is to compare various blends of WCO and select the most suitable fuel for
 449 the diesel engine. Here, B20 blend and EGR variation in B20 fuels have been taken as base fuels and

450 compared with diesel, B40, B60, and B100. A color code varying from red, yellow, and green in fig.
451 16 depicts the percentage variation in emission values. The negative values in fig. 16 represents the
452 increase in emission values while the positive values depict the decrease in emissions. Sharp
453 increase in emission is coded as red while sharp decrease as green and yellow means moderate in
454 variation. The analysis is done only for no load, part load, and full load conditions since 25% load
455 values did not vary much with no load and similarly part load with 75 % load condition. From the
456 previous sections, B20 blend fuel performed well in reducing various emissions like HC, CO, Smoke,
457 and CO₂. Now, the first column has been considered for comparison to comment on B20 blend fuel.
458 More negative values are seen at NO_x emission while a few for CO₂ at full load, smoke at full load
459 and CO at no load which has minor variations less than 7% except for CO showing -50% in
460 comparison with B100 (reason quoted in CO emission section). Since the fuel is burnt completely
461 producing high combustion temperature, B20 produces more NO_x emission in comparison with all
462 the other fuels. To prevent this NO_x emission, EGR has been introduced at 5, 10, and 15% variation.
463 EGR reduces NO_x while it raises emissions like CO, HC, Smoke, and CO₂. So, optimizing EGR
464 percentage is essential. Now, the other three columns except the first one have been considered
465 for further analysis. With 5% EGR rate, reduction in NO_x has occurred from B20 but still in
466 comparison with the other fuels there are many negative values in the figure. With 10% EGR rate,
467 the conversion has only positive values in the figure with a maximum reduction of 16.34%, while
468 the other emissions at this column (3rd column), have many positive values with a few negative
469 values of minor variations except in the case of CO at low and part loads. With 15% EGR rate,
470 reduction in NO_x is better than 10% rate with a maximum reduction of 21.05%, while the other
471 emissions at this column (4th column), have many negative values with a few positive values of
472 minor variations. Finally, considering all the columns B20 fuel with 10% EGR rate is found to be
473 better suited to the test engine.

Table 8 Emission variation summary

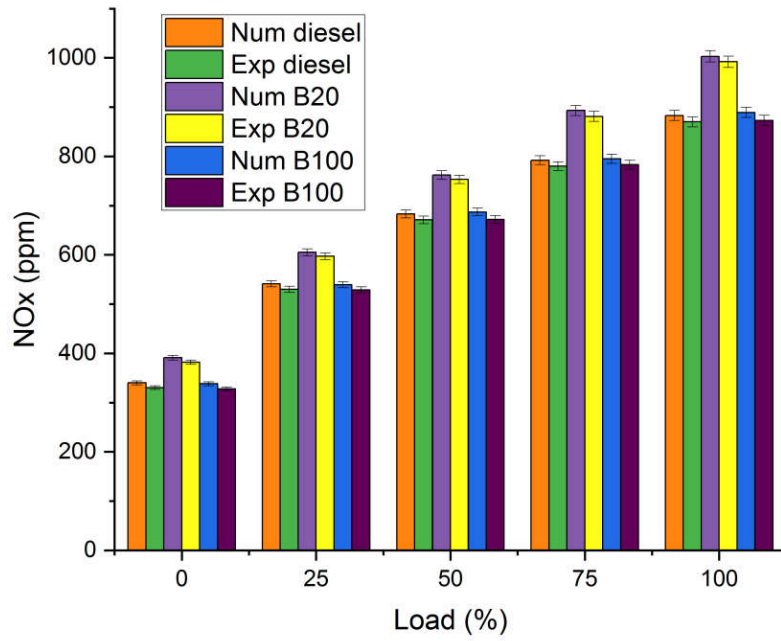
Emission	Load	Fuel	B20	B20 5% EGR	B20 10%	B20 15% EGR
CO	No load	Diesel	25.00	20.00	5.00	-5.00
		B40	-7.14	-14.29	-35.71	-50.00
		B60	-15.38	-23.08	-46.15	-61.54
		B100	-50.00	-60.00	-90.00	-110.00
	Part load	Diesel	10.00	8.00	2.00	-2.00
		B40	-7.14	-9.52	-16.67	-21.43
		B60	-12.50	-15.00	-22.50	-27.50
		B100	-18.42	-21.05	-28.95	-34.21
	Full load	Diesel	30.00	20.00	10.00	5.00
		B40	12.50	0.00	-12.50	-18.75
		B60	22.22	11.11	0.00	-5.56
		B100	22.22	11.11	0.00	-5.56
HC	No load	Diesel	6.82	4.55	2.27	0.00
		B40	2.38	0.00	-2.38	-4.76
		B60	0.00	-2.44	-4.88	-7.32
		B100	4.65	2.33	0.00	-2.33
	Part load	Diesel	14.29	11.43	5.71	2.86
		B40	6.25	3.13	-3.12	-6.25
		B60	9.09	6.06	0.00	-3.03
		B100	11.76	8.82	2.94	0.00
	Full load	Diesel	17.07	15.85	12.20	9.76
		B40	5.56	4.17	0.00	-2.78
		B60	9.33	8.00	4.00	1.33
		B100	13.92	12.66	8.86	6.33
NOx	No load	Diesel	-15.76	2.73	8.48	13.64
		B40	-5.82	11.08	16.34	21.05
		B60	-11.70	6.14	11.70	16.67
		B100	-16.46	2.13	7.93	13.11
	Part load	Diesel	-12.22	-2.38	3.43	9.54
		B40	-5.76	3.51	8.99	14.75
		B60	-8.03	1.43	7.03	12.91
		B100	-12.05	-2.23	3.57	9.67
	Full load	Diesel	-14.02	-1.26	1.95	7.01
		B40	-4.20	7.46	10.40	15.02
		B60	-10.10	2.22	5.33	10.21
		B100	-13.63	-0.92	2.29	7.33
Smoke	No load	Diesel	-14.57	-15.89	-19.87	-24.50
		B40	10.36	9.33	6.22	2.59
		B60	20.64	19.72	16.97	13.76
		B100	31.35	30.56	28.17	25.40
	Part load	Diesel	-13.41	-14.82	-16.47	-17.88
		B40	2.63	1.41	0.00	-1.21
		B60	8.02	6.87	5.53	4.39
		B100	14.08	13.01	11.76	10.70

	Full load	Diesel	4.99	4.56	3.72	3.08
		B40	-2.29	-2.74	-3.66	-4.34
		B60	-3.59	-4.05	-4.98	-5.67
		B100	-4.80	-5.27	-6.21	-6.91
CO ₂	No load	Diesel	-5.56	-6.11	-7.22	-10.00
		B40	2.56	2.05	1.03	-1.54
		B60	9.52	9.05	8.10	5.71
		B100	13.64	13.18	12.27	10.00
	Part load	Diesel	-1.61	-2.26	-3.23	-4.52
		B40	1.56	0.94	0.00	-1.25
		B60	4.55	3.94	3.03	1.82
		B100	7.35	6.76	5.88	4.71
	Full load	Diesel	-1.96	-3.73	-4.51	-5.29
		B40	-1.96	-3.73	-4.51	-5.29
		B60	-4.00	-5.80	-6.60	-7.40
		B100	-6.12	-7.96	-8.78	-9.59

475

476 4.2.8 Numerical and Experimental Comparison

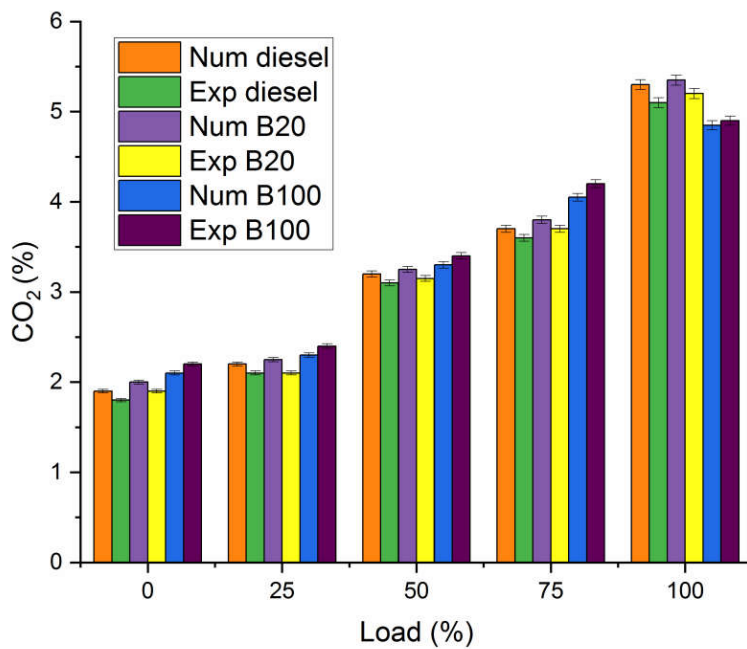
477 The simulation was carried out by using Ansys Fluent software and the results were predicted
478 for the mass fraction of NO_x and CO₂ emissions. The predicted results of NO_x emission for the
479 blend B20 showed an increase of 16.9% and 17.6% in comparison with diesel and B100 fuel
480 respectively. The experimental results of NO_x emission for the blend B20 showed a highest increase
481 of 15.76% and 16.46% in comparison with diesel and B100 fuel respectively. The simulated results
482 showed higher percentage variation than the experimental results and it is represented in the fig 17.
483 The error occurred was around +6.7% between the numerical and experimental comparison for NO_x
484 emission. The predicted results of CO₂ emission for the blend B20 showed an increase of 5.8% with
485 diesel and a decrease of 12.52% in comparison with B100 fuel. The experimental results of CO₂
486 emission for the blend B20 showed an increase of 5.5% with diesel and a decrease of 13.46% in
487 comparison with B100 fuel. The error occurred was around ±6.9% between the numerical and
488 experimental comparison for CO₂ emission. The fig. 18 depicts the numerical and experimental
489 values of CO₂ emission at various load conditions. Thus the error occurred was within the acceptable
490 limits.



491

492

Fig. 17 Numerical vs Experimental NOx emissions



493

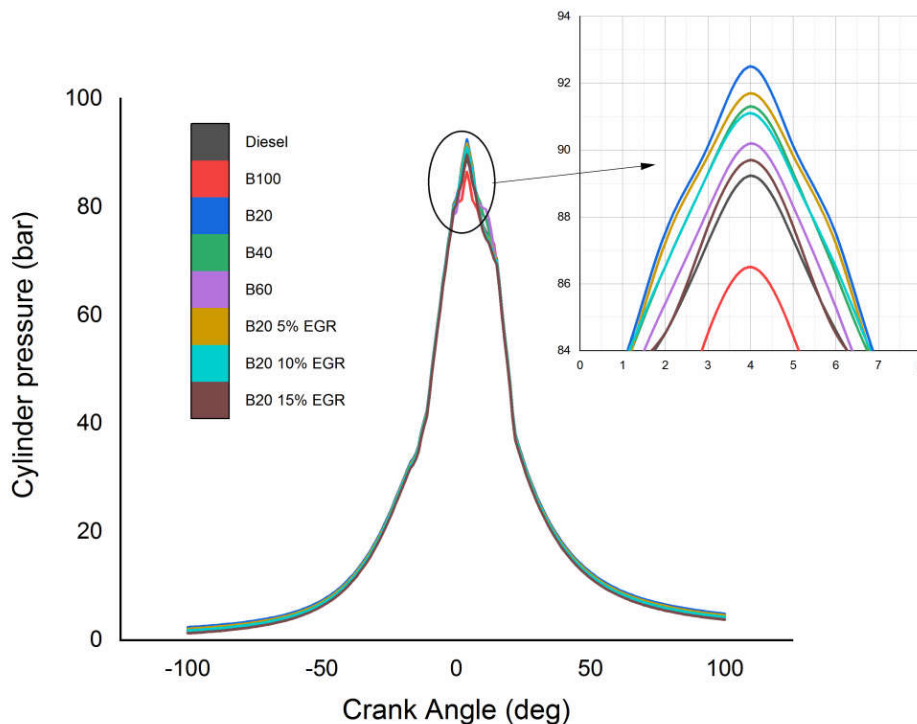
494

Fig. 18 Numerical vs Experimental CO2 emissions

495 **4.3 Combustion Characteristics**

496 **4.3.1 In-Cylinder Pressure**

497 Fig. 19 represents the variation in in-cylinder pressure with crank angle for all WCO blends,
498 diesel, and WCO biofuel at fuller load condition. The burning capability of fuel along with the mixing
499 of air characterizes cylinder pressure. The obtained peak cylinder pressure values are 89.2, 86.5,
500 90.2, 91.3, and 92.5 bar for diesel, B100, B60, B40, and B20 respectively. This trend shows that B20
501 blend has high peak pressure when compared with all the blends thus increasing the in-cylinder
502 pressure as discussed in the previous sections. All blends and WCO diesel follow similar trend of
503 diesel in the cylinder pressure which indicates that WCO fuel is suitable for this engine. Introduction
504 of EGR has decreased the cylinder pressure in the B20 blend fuel. The reason is increase in heat
505 capacity of inlet mixture and reduction in availability of oxygen [37], thus affecting the burning rate
506 and reducing pressure inside the cylinder. This results in the reduction in CO₂ and H₂O because of
507 an endothermic reaction leading to reduced NO_x.

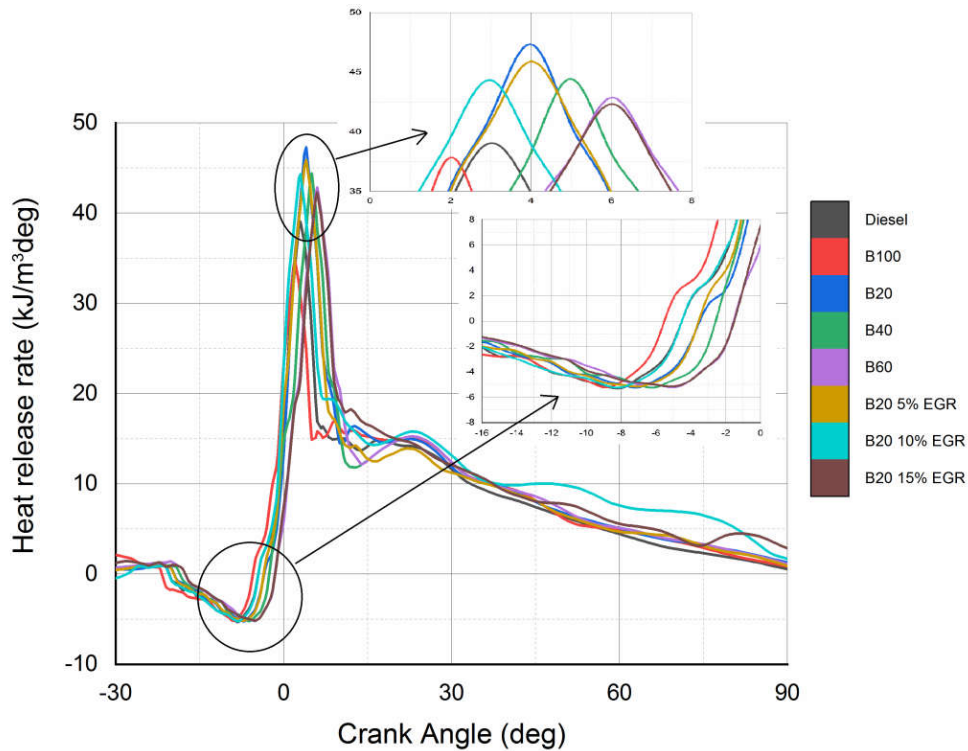


508

509 **Fig. 19 Crank angle Vs In-cylinder pressure**

510 **4.3.2 Heat Release Rate**

511 Fig. 20 depicts HRR variation with crank angle for all WCO blends, diesel, and WCO biofuel at
512 fuller load condition. This graph defines the various combustion related parameters like ignition
513 delay period, start of combustion, start of ignition and fuel quantity getting ignited at premixed
514 stage of combustion. There are two stages in combustion, namely premixed stage and diffusion
515 stage. The two stages of combustion have been separately shown in fig 18. Two different peaks in
516 the curve with initial one representing the premixed stage and the consecutive peak representing
517 the diffusion stage of combustion [38]. The negative values in the curve depict the fuel evaporation.
518 At full load, the obtained peak HRRs are 39.06, 36.83, 42.85, 44.42, and 47.32 kJ/m³deg for diesel,
519 B100, B60, B40, and B20 respectively. All types of blends have exhibited similar trend with respect
520 to diesel HRR curve. WCO biofuel and diesel show lower HRR when compared with WCO blends,
521 while in diesel ignition occurs soon due to higher calorific value of diesel and in the case of WCO
522 biofuel, beyond higher oxygen content in the fuel, it has released lesser HRR due to shorter ignition
523 delay period. B20 blend fuel has exhibited high HRR when compared with all the other types of
524 blends. The reason behind could be longer delay period. The sufficient oxygen content in the fuel
525 helped the diesel to burn effectively inside the cylinder to produce high combustion chamber
526 temperature. Also the duration of diffusion stage is higher thus facilitating better burning of
527 mixture of fuel and air. Rise in EGR in B20 blend decreases HRR. The reason behind this is reduced
528 temperature of combustion caused by poor atomization and reduced rate of air-fuel mixing with
529 B20 blend [37].



530

531

Fig. 20 Crank angle vs Heat release rate

532

4.3.3 Combustion noise

533

534

535

536

537

538

539

540

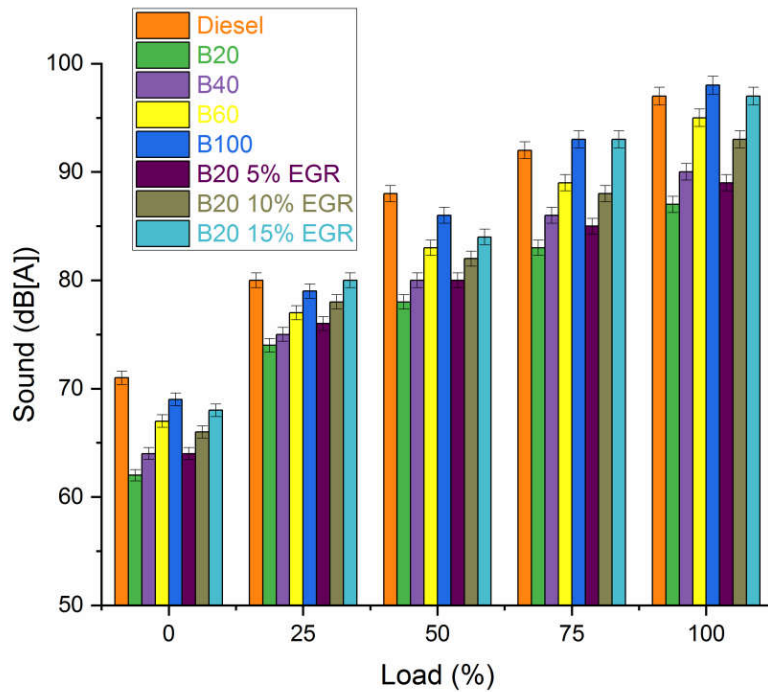
541

542

543

Fig. 21 represents the sound level variation along with the increase in engine load for all types of test fuels. The major amount of noise arising from CI engines is noise during combustion which occurs because of combustion of fuel taking place inside the combustion chamber. The noise could be sensed because of the pressure variation inside the cylinder [39]. At part load condition, the noise levels obtained are 88, 86, 83, 80, and 78 dB[A] for diesel, B100, B60, B40, and B20 respectively. The trend shows that B20 blend has lower noise level when it is compared with all the other blends since increasing in-cylinder pressure causes complete combustion while other blends show more pressure fluctuations because of incomplete combustion leading to more noise and at 100% load condition, the obtained noise levels are 97, 98, 95, 90, and 87 dB[A] for diesel, B100, B60, B40, and B20 respectively. Similar trend is followed by B20 but while comparing B100 with diesel, there is a slight increase in the noise level for B100. It is due to high oxygen content quenching the

544 flame causing incomplete combustion and pressure variation inside the cylinder. Introduction of
545 EGR increases the noise level in B20 blend fuel. It is because of increase in the heat capacity of the
546 inlet mixture and reduction in oxygen availability [37]. Thus affecting the combustion rate and
547 fluctuating the in-cylinder pressure.



548

549

Fig. 21 Load Vs Sound

550 **5. Conclusion**

551 In this current research, WCO biofuel was obtained using trans-esterification method and its
552 chemical constituents were determined using GCMS method. WCO biofuel was then blended with
553 diesel in varying quantities like 20%, 40%, and 60%. The fuel properties were determined by using
554 ASTM standards. With all the test fuels, performance, emission, combustion, and noise
555 characteristics were determined by using 4-stroke, two cylinder, D.I. diesel engine fitted along with
556 electrical dynamometer. B20 blend was found to be the best suitable fuel with respect to various

557 characteristics of the test engine. Fuel combustion modeling was also carried out using ANSYS
558 Fluent software for diesel, B20, and B100 fuels to predict temperature profile and mass fraction of
559 NO_x and CO₂. The predicted results are well in accordance with the experimental results. To control
560 NO_x, EGR was used in the selected blend fuel at varying rates of 5%, 10%, and 15%. The following
561 conclusions were drawn from the current research work:

- 562 ● At all load conditions, B20 blend showed reduced BTE with a maximum of 1.85% at full
563 load with respect to diesel while an increase in BTE with a maximum of 4.92, 4.49, and
564 3.87% at full load for B100, B60, and B40 respectively. The reason was due to high calorific
565 value, low viscosity in comparison with the other WCO blends. EGR addition decreased BTE
566 because of reduced flame temperature. Both 5% and 10% EGR rates showed better
567 performance in comparison with B40, B60, and B100 while 15% EGR rate showed reduced
568 BTE at all load conditions.
- 569 ● At all load conditions, B20 blend showed increased SFC with a maximum of 6.89% with
570 respect to diesel while reduced SFC with a maximum of 12.5, 14.4, and 15.2% at no load
571 with respect to B40, B60, and B100. EGR addition increased SFC because of excess fuel
572 need to maintain the power. Both 5% and 10% EGR rates showed reduced SFC in
573 comparison with B40, B60, and B100 while 15% EGR rate showed increased SFC at all load
574 conditions.
- 575 ● B20 blend fuel showed high HRR and in-cylinder pressure when compared with all the
576 other test fuels. This might be due to the availability of sufficient O₂ to burn diesel which
577 simultaneously increased the combustion flame temperature. With the addition of EGR,
578 cylinder pressure and HRR decreased. This was attributable to the reduction in oxygen
579 availability and reduced rate of air-fuel mixture.

- 580 • B20 blend showed reduced noise level at all load conditions in comparison with all the
581 other types of test fuels. This could be attributed to reduced pressure fluctuations inside
582 the engine. With EGR addition, noise level increased due to the presence of pressure
583 variations.
- 584 • With respect to the emission parameters like HC, CO, Smoke, NO_x, and CO₂, a separate
585 table was provided in the previous section which explained that B20 with 10% EGR rate
586 was selected as most suitable fuel with a good reduction in NO_x emissions without
587 affecting HC, CO, Smoke, and CO₂ emissions.

588 From the current research work, it can be stated that B20 blend fuel would be an optimum fuel
589 to enhance combustion, performance, sound and emission parameters (except NO_x) of test engine.
590 Further to reduce NO_x emission, B20 with 10% EGR rate would be selected as optimum rate
591 without affecting much combustion and performance parameters of the test engine.

592 **Acknowledgement**

593 The authors would like to thank CIT - Atalon Engine Research Center for providing the
594 experimental facilities through out the research work. The authors would also like to acknowledge
595 the management of Mepco Schlenk Engineering College for encouraging the research work.

596 **Conflicts of interest**

597 The authors declare that they have no known competing financial interests or personal
598 relationships that could have appeared to influence the work reported in this paper.

599 **References**

- 600 [1] R.B. Sharma, Amit Pal, Juhi Sharaf. Production of bio-diesel from waste cooking-oil, J. Eng. Res.
601 Appl. 4 (6) (2013) 1629–1636.

- 602 [2] C. Oner, S. Altun. biofuel production from inedible animal tallow and an experimental
603 investigation of its use as alternative fuel in a direct injection diesel engine, *J. Appl. Energy* 86 (2009)
604 2114–2120.
- 605 [3] Aninidita Karmakar. Properties of various plants and animals feedstocks for biofuel production,
606 *Bioresource Technology* 101 (2010) 7201–7210.
- 607 [4] S. Kent Hoekman. Review of biofuel composition, properties, and specifications, *Renewable and*
608 *Sustainable Energy Reviews* 16 (2012) 143– 169.
- 609 [5] EkremBuyukkaya, SerdarBenli, SalihKaraaslan, Metin Guru. Effects of trout-oil methyl ester on a
610 diesel engine performance and emission characteristics, *Energy Conversion and Management* 69
611 (2013) 41–48.
- 612 [6] F. Mohamed Al-Dawody. Theoretical study for the influence of biofuel addition on the
613 combustion, performance, and emissions parameters of single cylinder diesel engine, *J. Babylon*
614 *Univ. Pure Appl. Sci.* 26 (3) (2017) 57–69.
- 615 [7] Devendra Singh, S.K. Singal, M.O. Garg, Pratyush Maiti, Sandhya Mishra, Pushpito K. Ghosh,
616 Transient performance and emission characteristics of a heavy-duty diesel engine fuelled with
617 microalga *Chlorella variabilis* and *Jatropha curcas* biofuels, *Energy Convers. Manag.* 106 (2015)
618 892-900.
- 619 [8] Karavalakis G, Boutsika V, Stournas S, Bakeas E. biofuel emissions profile in modern diesel
620 vehicles. Part 2: effect of biofuel origin on carbonyl, PAH, nitroPAH and oxy-PAH emissions. *Sci Total*
621 *Environ* 2011;409(4):738–47. <https://doi.org/10.1016/j.scitotenv.2010.11.010>.

- 622 [9] Cheung CS, Zhu L, Huang Z. Regulated and unregulated emissions from a diesel engine fueled
623 with biofuel and biofuel blended with methanol. *Atmos Environ* 2009;43(32):4865–72.
624 <https://doi.org/10.1016/j.atmosenv.2009.07.021>.
- 625 [10] Kanakraj S, Rehman A, Dixit S. CI engine performance characteristics and exhaust emissions
626 with enzymatic degummed linseed methyl esters and their diesel blends. *Biofuels* 2017;8(3):347–
627 57.
- 628 [11] Mofijur M, Masjuki HH, Kalam MA, Atabani AE, Rizwanul Fattah IM, Mobarak HM. Comparative
629 evaluation of performance and emission characteristics of Moringa oleifera and Palm oil based
630 biofuel in a diesel engine. *Ind Crops Prod* 2014;53:78–84.
- 631 [12] Mofijur M, Masjuki HH, Kalam MA, Atabani AE, Arbab MI, Cheng SF, et al. Properties and use of
632 Moringa oleifera biofuel and diesel fuel blends in a multicylinder diesel engine. *Energy Convers*
633 *Manage* 2014;82:169–76.
- 634 [13] Kumar S, Cho JH, Park J, Moon II. Advances in diesel–alcohol blends and their effects on the
635 performance and emissions of diesel engines. *Renew Sustain Energy Rev* 2013;22:46–72.
- 636 [14] Zaharin MSM, Abdullah NR, Najafi G, Sharudin H, Yusaf T. Effects of physicochemical properties
637 of biofuel fuel blends with alcohol on diesel engine performance and exhaust emissions: a review.
638 *Renew Sustain Energy Rev* 2017;79:475–93.
- 639 [15] Atmanli A. Comparative analyses of diesel–waste oil biofuel and propanol, nbutanol or
640 1-pentanol blends in a diesel engine. *Fuel* 2016;176:209–15.
- 641 [16] Wei L., Cheung C.S., Ning Z. Influence of waste cooking oil biofuel on combustion, unregulated
642 gaseous emissions and particulate emissions of a direct-injection diesel engine. *Energy*,
643 2017;127:175-185.

- 644 [17] Carlos Daniel Mandolesi de Araújo, Claudia Cristina de Andrade, Erika de Souza e Silva,
645 Francisco Antonio Dupas. biofuel production from used cooking oil: A review. *Renewable and*
646 *Sustainable Energy Reviews*, 2013;27:445-452.
- 647 [18] Di Y, Cheung CS, Huang Z. Experimental investigation on regulated and unregulated emissions
648 of a diesel engine fueled with ultra-low sulfur diesel fuel blended with biofuel from waste cooking
649 oil. *Sci Total Environ* 2009;407:835–46.
- 650 [19] Cheung CS, Zhu L, Huang Z. Regulated and unregulated emissions from a diesel engine fueled
651 with biofuel and biofuel blended with methanol. *Atmos Environ* 2009;43:4865–72.
- 652 [20] Rajesh kumar B and Saravanan S. Effect of exhaust gas recirculation (EGR) on performance and
653 emissions of a constant speed DI diesel engine fueled with pentanol/diesel blends. *Fuel* 160
654 (2015):217–226. <http://dx.doi.org/10.1016/j.fuel.2015.07.089>.
- 655 [21] Zheng M, Mulenga MC, Reader GT, Wang M, Ting DSK, and Tjong J. biofuel engine performance
656 and emissions in low temperature combustion. *Fuel* 87(6) (2008):714–722.
- 657 [22] Lee K, Kim H, Park P, Yang S, and Ko Y. CO₂ radiation heat loss effects on NO_x emissions and
658 combustion instabilities in lean premixed flames. *Fuel* 106 (2013): 682–689.
- 659 [23] Chen Z, Liu J, Wu Z, and Lee C. Effects of port fuel injection (PFI) of n-butanol and EGR on
660 combustion and emissions of a direct injection diesel engine. *Energy Conversion and Management*
661 76 (2013):725–731.
- 662 [24] Noor MM, Wandel AP, and Yusaf T. Effect of air-fuel ratio on temperature distribution and
663 pollutants for biogas mild combustion. *International Journal of Automotive and Mechanical*
664 *Engineering* 10(1) (2014):1980–1992.

- 665 [25] Das LM, and Mathur R. Exhaust gas recirculation for Nox control in a multicylinder
666 hydrogen-supplemented S.I. engine. *International Journal of Hydrogen Energy* 18(12) (1993):1013–
667 1018.
- 668 [26] Kusaka J. Combustion and exhaust gas emission characteristics of a diesel engine dual- fueled
669 with natural gas. *JSAE Review* 21 (2000): 489–496.
- 670 [27] Agarwal D, Singh SK, and Agarwal AK. Effect of Exhaust Gas Recirculation (EGR) on
671 performance, emissions, deposits and durability of a constant speed compression ignition engine.
672 *Applied Energy* 88(8) (2011):2900–2907.
- 673 [28] Rajesh Govindan, O.P. Jakhar, Y.B. Mathur, Computational analysis of Thumba biofuel-diesel
674 blends combustion in CI engine using Ansys-fluent, *IJCMS* 3 (2014) 29–39.
- 675 [29] Norrizam Jaat et al., Analysis of injection pressure and high ambient density of biofuel spray
676 using computational fluid dynamics, *Combustion* 11 (1) (2019) 28–39.
- 677 [30] Moffat RJ. Using uncertainty analysis in the planning of an experiment. *J Fluids Eng*
678 1985;107(2):173–8. <https://doi.org/10.1115/1.3242452>.
- 679 [31] S. Dixit, A. Kumar, S. Kumar et al., CFD analysis of biofuel blends and combustion using Ansys
680 Fluent, *Materials Today: Proceedings*, <https://doi.org/10.1016/j.matpr.2019.12.362>.
- 681 [32] K.A. Abed, A.K. El Morsi , M.M. Sayed, A.A. El Shaib, M.S. Gad., Effect of waste cooking-oil
682 biofuel on performance and exhaust emissions of a diesel engine, *Egyptian Journal of Petroleum* 27
683 (2018) 985–989. <https://doi.org/10.1016/j.ejpe.2018.02.008>.
- 684 [33] K. Nantha Gopal, Arindam Pal, Sumit Sharma, Charan Samanchi, K. Sathyanarayanan, T. Elango,
685 Investigation of emissions and combustion characteristics of a CI engine fueled with waste cooking

686 oil methyl ester and diesel blends, Alexandria Engineering Journal (2014) 53, 281–287.
687 <http://dx.doi.org/10.1016/j.aej.2014.02.003>.

688 [34] Mohamed F. Al-Dawody, Ali A. Jazie, Hassan Abdulkadhim Abbas, Experimental and simulation
689 study for the effect of waste cooking oil methyl ester blended with diesel fuel on the performance
690 and emissions of diesel engine, Alexandria Engineering Journal (2019) 58, 9–17.
691 <https://doi.org/10.1016/j.aej.2018.05.009>.

692 [35] S. Senthur Prabu, M.A. Asokan, Rahul Roy, Steff Francis, M.K. Sreelekh, Performance,
693 Combustion and Emission Characteristics of Diesel Engine fuelled with Waste Cooking Oil Bio-diesel
694 or diesel blends with Additives, Energy (2017), <https://doi.org/10.1016/j.energy.2017.01.119>.

695 [36] X.J. Man, C.S. Cheung, Z. Ning, L. Wei, Z.H. Huang, Influence of engine load and speed on
696 regulated and unregulated emissions of a diesel engine fueled with diesel fuel blended with waste
697 cooking oil biofuel, Fuel 180 (2016) 41–49. <https://dx.doi.org/10.1016/j.fuel.2016.04.007>.

698 [37] De Serio, D., de Oliveira, A., & Sodre, J. R., Effects of EGR rate on performance and emissions of
699 a diesel power generator fueled by B7. Journal of the Brazilian Society of Mechanical Sciences and
700 Engineering, 39(6), 1919–1927 (2017). <https://doi.org/10.1007/s40430-017-0777-x>.

701 [38] V. Karthickeyan, S. Thiyagarajan, V. Edwin Geo, B. Ashok , K. Nanthagopal, Ong Hwai Chyuan , R.
702 Vignesh, Simultaneous reduction of NOx and smoke emissions with low viscous biofuel in low heat
703 rejection engine using selective catalytic reduction technique, Fuel 255 (2019) 115854.
704 <https://doi.org/10.1016/j.fuel.2019.115854>.

705 [39] Tüccar G. Effect of hydroxy gas enrichment on vibration, noise and combustion characteristics
706 of a diesel engine fueled with Foeniculum vulgare oil biofuel and diesel fuel. Energy Sources, Part A
707 Recover Util Environ Eff 2018;00:1–9. <https://doi.org/10.1080/15567036.2018.1476622>.

- 708 [40] Balasubramanian, D., Venugopal, I. P., & Viswanathan, K. (2019). Characteristics Investigation
709 on Di Diesel Engine with Nano-Particles as an Additive in Lemon Grass Oil (No. 2019-28-0081). SAE
710 Technical Paper.
- 711 [41] Dhinesh Balasubramanian, Sriram Kamaraj, R Krishnamoorthy.(2020). Synthesis of biofuel from
712 Waste Cooking Oil by Alkali Doped Calcinated Waste Egg Shell Powder Catalyst and Optimization of
713 Process Parameters to Improve biofuel Conversion (No. 2020-01-0341) SAE Technical Paper.
- 714 [42] Inbanaathan P.V., Dhinesh B., Tamilarasan U. (2020) Experimental Investigation of
715 Performance and Emission Characteristics of Diesel Blended with Palm Methyl Ester Along with
716 Alumina Nano-Additive Using D.I. Diesel Engine. In: Ghosh S., Sen R., Chanakya H., Pariatamby A.
717 (eds) Bioresource Utilization and Bioprocess. Springer, Singapore
- 718 [43] Karthickeyan V., Dhinesh B., Balamurugan P. (2020) Effect of Compression Ratio on
719 Combustion, Performance and Emission Characteristics of DI Diesel Engine with Orange Oil Methyl
720 Ester. In: Ghosh S., Sen R., Chanakya H., Pariatamby A. (eds) Bioresource Utilization and Bioprocess.
721 Springer, Singapore.
- 722 [44] Desantes JM, Galindo J, Guardiola C, Dolz V. Air mass flow estimation in turbocharged diesel
723 engine from in-cylinder pressure measurement. *Exp Therm Fluid Sci* 2010;34:37–47.
- 724 [45] M.S. Gad, Ahmed I. EL-Seesy, Ali Radwan , Zhixia He. Enhancing the combustion and emission
725 parameters of a diesel engine fueled by waste cooking oil biodiesel and gasoline additives. *Fuel* 269
726 (2020) 117466. <https://doi.org/10.1016/j.fuel.2020.117466>.
- 727 [46] Mohamed Nour, Ahmed I. EL-Seesy, Ali K. Abdel-Rahman, Mahmoud Bady. Influence of Adding
728 Aluminum Oxide Nanoparticles to Diesterol Blends on the Combustion and Exhaust Emission

729 Characteristics of a Diesel Engine. *Experimental Thermal and Fluid Science*, S0894-1777(18)30821-5.
730 <https://doi.org/10.1016/j.expthermflusci.2018.07.009>.

731 [47] Ahmed I. El-Seesy, Ali M.A. Attia, Hesham M. El-Batsh. The effect of Aluminum oxide
732 nanoparticles addition with Jojoba methyl ester-diesel fuel blend on a diesel engine performance,
733 combustion and emission characteristics. *Fuel* 224 (2018) 147–166.
734 <https://doi.org/10.1016/j.fuel.2018.03.076>.

735 [48] Meshack Hawi, Ahmed Elwardany, Shinichi Ookawara, Mahmoud Ahmed. Effect of
736 compression ratio on performance, combustion and emissions characteristics of compression
737 ignition engine fueled with jojoba methyl ester. *Renewable Energy* 141 (2019) 632-645.
738 <https://doi.org/10.1016/j.renene.2019.04.041>.

739 [49] Ramalingam, K., Balasubramanian, D., Chellakumar, P. J. T. J. S., Padmanaban, J., Murugesan, P.,
740 & Xuan, T. (2020). An assessment on production and engine characterization of a novel
741 environment-friendly fuel. *Fuel*, 279, 118558.

742 [50] EL-Seesy, A. I., He, Z., Hassan, H., & Balasubramanian, D. (2020). Improvement of combustion
743 and emission characteristics of a diesel engine working with diesel/jojoba oil blends and butanol
744 additive. *Fuel*, 279, 118433.

745 [51] Gao, J., Tian, G., Ma, C., Balasubramanian, D., Xing, S., & Jenner, P. (2020). Numerical
746 investigations of combustion and emissions characteristics of a novel small scale opposed rotary
747 piston engine fuelled with hydrogen at wide open throttle and stoichiometric conditions. *Energy*
748 *Conversion and Management*, 221, 113178.

- 749 [52] Nagarajan Jeyakumar, Bose Narayanasamy, Dhinesh Balasubramanian, V. Karthickeyan (2020).
750 Characterization and effect of Moringa Oleifera Lam. antioxidant additive on the storage stability of
751 Jatropha biodiesel. Fuel, 279, 118614.
- 752 [53] Hoang, A. T., Tabatabaei, M., Aghbashlo, M., Carlucci, A. P., Ölçer, A. I., Le, A. T., & Ghassemi, A.
753 Rice bran oil-based biodiesel as a promising renewable fuel alternative to petrodiesel: A
754 review. Renewable and Sustainable Energy Reviews, 135, 110204.
- 755 [54] Hoang, A. T., & Pham, V. V. (2019). A study of emission characteristic, deposits, and lubrication
756 oil degradation of a diesel engine running on preheated vegetable oil and diesel oil. Energy Sources,
757 Part A: Recovery, Utilization, and Environmental Effects, 41(5), 611-625.
- 758 [55] Hoang, A. T., & Le, A. T. (2019). A core correlation of spray characteristics, deposit formation,
759 and combustion of a high-speed diesel engine fueled with Jatropha oil and diesel fuel. Fuel, 244,
760 159-175.

761

762 **Nomenclature**

763 BTE - Brake Thermal Efficiency (%)

764 SFC - Specific Fuel Consumption (kg/kWhr)

765 WCO - Waste Cooking Oil

766 EGR - Exhaust Gas Recirculation

767 CI - Compression Ignition

768 ASTM - American Standards for Testing and Materials

- 769 DI - Direct Injection
- 770 HC - Hydrocarbon (ppm)
- 771 CO - Carbon monoxide (% vol)
- 772 NO_x - Oxides of nitrogen (ppm)
- 773 CO₂ - Carbon dioxide (% vol)
- 774 GCMS - Gas Chromatography Mass Spectroscopy method
- 775 HRR - Heat Release Rate (kJ/m³deg)
- 776 CP - Cylinder Pressure (bar)
- 777 B20 - 20% WCO biofuel and 80% diesel
- 778 B40 - 40% WCO biofuel and 60% diesel
- 779 B60 - 60% WCO biofuel and 40% diesel
- 780 B100 - 100% WCO biofuel
- 781 **Annexure**
- 782 GCMS results obtained for WCO and WCO biofuel are represented in fig.22